Flow Physics of Micro Particles Suspended in Viscoelastic Fluid in a Microchannel

M.Tech. Thesis

by

PRITHVIRAJ SONI

DEPARTMENT OF MECHANICAL ENGINEERING (ME)
INDIAN INSTITUTE OF TECHNOLOGY INDORE
JUNE 2025

Flow Physics of Micro Particles Suspended in Viscoelastic Fluid in a Microchannel

A THESIS

Submitted in partial fulfilment of the requirements for the award of the degree

of

Master of Technology

by

PRITHVIRAJ SONI

DEPARTMENT OF MECHANICAL ENGINEERING (ME)
INDIAN INSTITUTE OF TECHNOLOGY INDORE
JUNE 2025

INDIAN INSTITUTE OF TECHNOLOGY INDORE

CANDIDATE'S DECLARATION

I hereby certify that the work which is being presented in the thesis entitled **Flow Physics of Micro Particles Suspended in Viscoelastic Fluid in a Microchannel** in the partial fulfillment of the requirements for the award of the degree of **MASTER OF TECHNOLOGY** and submitted in the **DEPARTMENT OF MECHANICAL ENGINEERING, Indian Institute of Technology Indore**, is an authentic record of my work carried out during the period from August 2023 to May 2025 under the supervision of Dr. Vijai Laxmi Assistant Professor and Dr. Harekrishna Yadav, Associate Professor, ME, Indian Institute of Technology Indore.

I have not submitted the matter presented in this thesis for the award of any other degree of this or any other institute.

07/07/2025
Signature of the student with date
Prithviraj Soni

This is to certify that the above statement made by the candidate is correct to the best of my knowledge.

Vijai Laxmi 07/07/2025
Signature of the Supervisor of
M.Tech. thesis #1 (with date)
Dr. Vijai Laxmi

Harekrishna Yadav 07/07/2025
Signature of the Supervisor of
M.Tech. thesis #2 (with date)
Dr. H.K. Yadav

Prithviraj Soni has successfully given his MTech. Oral Examination held on **26th May 2025**.

Vijai Laxmi Harekrishna Yadav
Signature(s) of Supervisor(s) of M.Tech. thesis
Date: 07/07/2025

Convener, DPGC
Date:07-07-2025

Type text here

ACKNOWLEDGEMENTS

I would like to express my heartfelt gratitude to my supervisors **Dr. Vijai Laxmi**, and **Dr. H. K. Yadav**, at IIT Indore, for their invaluable guidance, constant encouragement, and throughout the course of my M.Tech thesis. Their profound expertise and insightful mentorship have played a pivotal role in shaping the direction and quality of this research work.

I extend my sincere thanks to the **Project Semester Progress Committee (PSPC)** members — **Dr. H. K. Yadav**, **Dr. Satyanarayan Patel**, and **Dr. Ankur Miglani**—for their valuable time, constructive feedback, and thoughtful suggestions, which have significantly enhanced the quality and clarity of this thesis.

I am also thankful to my batch mates **Kartik Gupta**, **Kushagra Parihar**, **Anshul Kashyap**, **Aditya Girge**, **Vandana Gariya**, **Prashant Singh, Apram Bhati** and **Rasika Kalokhe** for their presence during the tenure of Masters be it academics or mental support, you guys were always there, pushing me to be the best version of myself for me and everyone around.

My sincere appreciation goes to **Nikhil Pandey, Abhishek Singh** and **Nisha Kumari** in our lab, for their consistent support, technical help, and collaborative spirit, which have contributed meaningfully to the successful completion of this research.

Finally, I wish to express my deep appreciation to my **family, friends, and colleagues** for their unwavering encouragement, patience, and understanding throughout this academic journey. Their support has been a constant source of strength and motivation.

Abstract

This thesis presents a detailed numerical investigation into the behavior of microparticles in viscoelastic fluid environments within microfluidic channels of varying geometries. The study aims to understand how channel design and fluid properties influence particle migration, focusing particularly on passive manipulation strategies driven by elastic lift forces. Using COMSOL Multiphysics 6.0, a simulation model was first developed and validated by replicating results from a previously published, experimentally verified study. The replicated outcomes closely matched the reported experimental trends, establishing the reliability of the simulation framework.

Following this validation, the channel geometry was systematically altered to explore the effects of various symmetric and asymmetric well configurations—such as rectangular, triangular, and curved cavities—on particle deviation and focusing efficiency. Simulations were conducted across a range of flow rates (20–40 μL/min) and PEO (polyethylene oxide) concentrations (500 ppm and 1000 ppm), with fixed particle size (4.8 μm) to mimic red blood cells. Results showed that increasing polymer concentration enhanced viscoelastic lift forces, leading to more pronounced lateral particle migration. Moreover, complex geometries, particularly those with sharp transitions like double-sided triangular wells, produced stronger elastic focusing effects compared to simpler or smoother designs.

The results reveal a strong quantitative relationship between polymer concentration, channel geometry, and particle migration. For instance, in channels with symmetric rectangular wells, increasing the PEO concentration from 500 ppm to 1000 ppm boosts the average particle deviation at the channel exit from around 15.4 μm to 16.0 μm at the highest flow rate. The number of wells also plays a decisive role: as the count rises from 11 to 26, the average deviation grows from about 7 μm to 15 μm at 500 ppm, and up to 16 μm at 1000 ppm. However, this effect begins to plateau beyond 26 wells, with only modest increases in deviation observed up to 36 wells. Pressure drop analysis further underscores the advantages of symmetric well shapes, which consistently produce lower hydrodynamic resistance (2.8 kPa at 500 ppm 20 μL/min and 5.5 kPa at 1000 ppm 40 μL/min) compared to asymmetric configurations which shows 3.1 kPa and 5.75 kPa, respectively.

TABLE OF CONTENTS

LIST OF FIGURES

LIST OF TABLES

NOMENCLATURE

a [μm]	Particle diameter
β	Retardation factor
c [ppm]	concentration
D_h [m]	Hydraulic diameter
D	Strain velocity tensor
ε	Rheological parameter of the PPT model
F_D [N]	Lift force
F_E [N]	Elastic force
F_L [N]	Drag force
γ [1/s]	Shear rate
h [μm]	Height
I	Unit tensor
λ [s]	The relaxation time of fluid
μ [kg/ms]	Dynamic viscosity
μ_p [kg/ms]	Polymer viscosity
μ_s [kg/ms]	Solvent viscosity
N_1 [Pa]	First normal stress difference
N_2 [Pa]	Second normal stress difference
p [Pa]	Pressure
K	Newtonian component of stress tensor
Q [m^3]	Average flow rate
ρ [kg/m^3]	Density
Re	Reynolds Number
t_f [s]	Characteristic time
τ [Pa]	Stress tensor

T_e	Viscoelastic component of stress tensor
u [m/s]	Velocity vector
U_m [m/s]	Averaged velocity
w [µm]	Width
Wi	Weissenberg number

Chapter 1

Introduction

The manipulation and control of microparticles in confined microfluidic environments represents a rapidly evolving field that bridges fundamental fluid mechanics with practical biomedical applications. This research explores the complex flow physics governing microparticle behavior when suspended in viscoelastic fluids within microchannel geometries, where the interplay between elastic forces, inertial effects, and channel confinement creates unique opportunities for precise particle manipulation [1, 2]. The study reveals how non-Newtonian fluid properties fundamentally alter particle migration patterns compared to conventional Newtonian systems, enabling enhanced focusing and separation capabilities that are increasingly vital for lab-on-a-chip applications, medical diagnostics, and biological research platforms [3].

1.1 Understanding Microfluidics: Foundation and Applications

Microfluidics represents both the science that studies the behavior of fluids through micro-channels and the technology for manufacturing microminiaturized devices containing chambers and tunnels through which fluids flow or are confined. This multidisciplinary field involves the manipulation and control of very small fluid volumes, typically ranging from microliters to femtoliters, within channels or devices with dimensions on the microscale[4]. The fundamental principle underlying microfluidics centers on the integration of multiple laboratory operations into a simple micro-sized system, effectively creating what researchers commonly refer to as "lab-on-a-chip" devices [4].

At the microscale, fluids exhibit dramatically different behaviors compared to their macroscopic counterparts, presenting unique opportunities for scientific innovation and experimentation. These distinctive characteristics arise from the dominance of surface forces over bulk forces, altered mixing mechanisms, and modified heat and mass transfer properties that emerge when characteristic lengths approach the micrometer scale [4].

The precise control afforded by microfluidic systems enables researchers to manipulate individual cells, particles, and molecules with unprecedented accuracy while consuming minimal reagent volumes.

Contemporary microfluidic applications span diverse fields, demonstrating the technology's versatility and transformative potential. Organ-on-a-chip systems represent one of the most promising applications, recreating organ functions to accelerate pharmaceutical research while reducing reliance on animal testing [5]. These devices enable researchers to study human organ responses to drugs, toxins, and diseases in controlled environments that closely mimic physiological conditions. Additionally, microfluidic cell sorting and separation technologies have achieved significant commercial success, operating on the basis of cellular parameter differences to achieve highly effective, modular, and cost-effective separation processes [6, 7]. Gene delivery applications further showcase microfluidic capabilities, where devices transfer genetic or chemical cargo into cells at higher efficiencies than traditional bulk methods [7].

1.2 Viscoelastic Fluids in Microfluidic Systems

The integration of viscoelastic fluids into microfluidic platforms has emerged as a transformative approach for particle manipulation, offering distinct advantages over conventional Newtonian fluid systems [1,8]. Viscoelastic materials exhibit both viscous and elastic characteristics when undergoing deformation, creating time-dependent strain responses that fundamentally alter fluid flow patterns and particle dynamics. In microfluidic contexts, these fluids typically consist of polymer solutions, such as polyethylene oxide (PEO) or polyvinylpyrrolidone (PVP), dissolved in aqueous media to create non-Newtonian flow characteristics [2].

The unique properties of viscoelastic fluids arise from their ability to store part of the energy transferred through deformation as elastic energy, resulting in materials that demonstrate intermediate behavior between liquid and solid states. This dual nature manifests through specific rheological properties characterized by storage and loss moduli, relaxation times, and normal stress differences that govern particle migration patterns within confined channels.

When viscoelastic fluids flow through microchannels, they generate non-uniform stress distributions that create lateral forces capable of manipulating suspended particles in ways impossible with purely viscous fluids.

Recent advances in viscoelastic microfluidics have demonstrated remarkable capabilities for single-stream three-dimensional focusing in simple channel geometries, eliminating the need for complex sheath flow systems or external force fields. The manipulation of cells and

particles suspended in these fluids has drawn increasing attention due to the field-free nature of the focusing mechanism, fast and simple operation procedures, and minimal sample consumption requirements. Multiple factors actively interact and compete to govern the intricate migration behavior of particles and cells, including driving forces arising from fluid elasticity and inertia, fluid rheology effects, physical properties of particles and cells, and channel geometry considerations [8].

1.3 Particle Focusing and Separation Applications

The application of viscoelastic fluids for particle focusing and separation represents a convergence of fundamental fluid mechanics and practical microfluidic technology, offering unprecedented control over microscale particle manipulation. In viscoelastic flows, particles experience elastic lift forces that arise from non-uniform normal stress distributions within the channel cross-section, driving particles toward specific equilibrium positions. These forces, governed by the first and second normal stress differences, create focusing effects that can be precisely controlled through fluid properties, flow conditions, and channel geometry [2,8].

The focusing mechanism in viscoelastic microfluidics operates through the balance of multiple competing forces, including elastic forces that drive particles toward the channel centerline, inertial forces that can create equilibrium positions near channel walls, and Dean forces in curved channels that provide additional lateral migration components [1, 2].

The relative magnitude of these forces, characterized by dimensionless parameters such as the Weissenberg number and Reynolds number, determines the final focusing positions and separation resolution achievable for particles of different sizes [2, 8]. Recent research has demonstrated that particles can be efficiently focused into single streams with focusing positions predictable through force balance analysis.

Enhanced separation capabilities have been achieved through optimized channel designs and operating conditions, with reported separation resolutions reaching 100 nanometers for synthetic particles and successful separation of biological entities such as extracellular vesicles [3]. Innovative approaches utilizing gradually contracted channel geometries have shown significant improvements in focusing efficiency, reducing required channel lengths while maintaining excellent focusing performance [8].

The versatility of viscoelastic particle manipulation extends to complex particle mixtures, where ternary separations of 100 nm, 200 nm, and 500 nm particles have been achieved with purities above 70% for each size fraction [9]. Furthermore, the technique has been successfully applied to biological samples, including the focusing and separation of white blood cells, red blood cells, and cancer cells, demonstrating its potential for clinical diagnostics and biomedical research applications. The combination of viscoelastic focusing with secondary separation mechanisms, such as magnetophoretic, has shown promise for achieving enhanced separation specificity and throughput [9].

Chapter 2

Literature Survey and Problem Formulation

2.1.1 Definition and Nature of Viscoelastic Fluids

Viscoelastic fluids represent a unique class of materials that exhibit both viscous and elastic properties when subjected to deformation or flow. These fluids demonstrate memory effects, where their response to applied stress depends not only on the current conditions but also on their deformation history [10]. Zhou and Papautsky define viscoelastic materials as those possessing elasticity due to the first normal stress difference (N_1) and/or shear-dependent viscosity, which can give rise to focusing of particles in such media [10].The elastic nature of these fluids arises from their molecular structure, particularly in polymer solutions where long-chain molecules can store and release elastic energy during deformation. This fundamental characteristic distinguishes viscoelastic fluids from simple Newtonian fluids and creates unique flow phenomena that have attracted considerable research attention in microfluidic applications [11, 12].

2.1.2 Components and Composition of Viscoelastic Fluids

Viscoelastic fluids are commonly formulated using two essential components: a solvent phase, which behaves in a Newtonian manner, and a polymer phase, which introduces the fluid's characteristic elasticity. Among the various polymers used in experimental studies, polyethylene oxide (PEO) is frequently chosen due to its well-documented rheological properties, ease of preparation, and excellent biocompatibility — making it suitable for a wide range of biological and microfluidic applications [10,11,12].

In a detailed experimental investigation, Yuan et al. explored the behavior of PEO solutions at varying concentrations — specifically between 500 to 5000 ppm — dissolved in deionized water. Their results highlighted the emergence of distinct viscoelastic characteristics as the polymer concentration increased [11]. The contribution of the polymer to the fluid's overall behavior is quantified through polymer viscosity (η_p), while the solvent contributes via solvent viscosity (η_s). Together, these combine to yield the total viscosity of the viscoelastic fluid, described by the simple relationship:

$$\eta = \eta_s + \eta_p \quad (11).$$

This equation captures the cooperative role of both components in determining the flow response of the fluid under various shear conditions. However, viscosity alone does not fully describe a viscoelastic fluid's behavior. Its properties are also heavily influenced by polymer molecular weight and concentration, which govern the fluid's elasticity and flow-induced stress responses. In this context, Hazra et al. performed an extensive study using polymer solutions with varying molecular weights: PEO at 1 and 4 MDa, polyacrylamide (PAM) at 5–6 MDa, and polyacrylic acid (PAA) at 4 MDa [12]. Notably, these polymers were tested at concentrations well above the critical overlap concentration (c*), a threshold at which polymer chains begin to interact and entangle. This strategic selection allowed the researchers to fine-tune viscoelastic properties, enabling more precise control over particle behavior within microfluidic flows - a key requirement for designing efficient separation and focusing devices.

2.1.3 Viscoelastic versus Newtonian Fluid Behavior

A core difference between viscoelastic and Newtonian fluids lies in how they respond when subjected to mechanical stress - a response governed by their constitutive relationships. In the case of Newtonian fluids, such as water or air, this relationship is simple and linear: the shear stress is directly proportional to the shear rate, and the viscosity remains constant regardless of how fast or slow the fluid is deformed. This predictability is what makes Newtonian fluids mathematically convenient and intuitively easy to work with.

However, viscoelastic fluids behave quite differently. These fluids, often containing flexible polymer chains, exhibit complex rheological responses that evolve over time and vary with flow conditions. Instead of a constant viscosity, they often display shear-dependent viscosity - typically decreasing as the shear rate increases, a phenomenon known as shear-thinning. More importantly, viscoelastic fluids develop normal stress differences, which are stresses that act perpendicular to the direction of applied shear. These normal stresses have no equivalent in Newtonian systems and are a hallmark of elasticity in flowing polymer solutions [10].This unique combination of viscous damping and elastic memory makes viscoelastic fluids highly valuable in microscale applications, particularly in particle focusing and separation, where forces arising from these normal stress differences can be harnessed to manipulate particles without the need for external fields.

2.1.4 Rheological Characteristics

In its simplest form, a Newtonian fluid follows Newton's law of viscosity, which states that the

shear stress (τ) exerted by the fluid is directly proportional to the velocity gradient (du/dy) - the rate at which the fluid layers move past each other. The constant of proportionality in this relationship is the dynamic viscosity (μ), which remains unaffected by changes in flow conditions. Mathematically, this behavior is described as: $\tau = \mu(du/dy)$.

This linear and predictable nature makes Newtonian fluids straightforward to analyze, especially in engineering and physics applications where steady and uniform fluid behavior is desirable [10]. By contrast, viscoelastic fluids deviate from this simplicity in several important ways. One of the most prominent differences is their non-constant viscosity, which can vary significantly with shear rate. Some viscoelastic fluids exhibit shear-thinning behavior, where viscosity decreases as shear rate increases - a common trait in polymer solutions and biological fluids. Others may show shear-thickening, where viscosity increases with shear rate, though this is less common. These behaviors arise from the internal structure and dynamics of polymer chains suspended in the fluid, which stretch, align, or entangle depending on the flow conditions [10]. Another defining feature of viscoelastic fluids is the presence of normal stress differences, which are entirely absent in Newtonian fluids. These include the first normal stress difference ($N_1 = \tau_{xx} - \tau_{\gamma\gamma}$) and the second normal stress difference ($N_2 = \tau_{\gamma\gamma} - \tau_{zz}$). These stress components act perpendicular to the flow direction and are responsible for many of the elastic phenomena observed in microfluidics - such as particle migration, rod climbing, and die swell effects. Importantly, the first normal stress difference (N_1) plays a dominant role in generating elastic lift forces, which are central to particle focusing mechanisms in viscoelastic microflows [10, 12].

Together, these characteristics — nonlinear viscosity and normal stress development - form the rheological signature of viscoelastic fluids, setting them apart from their Newtonian counterparts and making them uniquely suited for advanced fluid manipulation in microscale environments.

2.1.5 Constitutive Models

To understand and predict how viscoelastic fluids behave under flow, researchers rely on constitutive models - mathematical frameworks that relate stress and deformation in complex fluids. Among the most widely used is the Oldroyd-B model, which serves as a foundational tool in viscoelastic fluid mechanics [13]. This model captures the essence of elastic effects by predicting the development of the first normal stress difference (N_1), a key driver of particle

migration in microfluidic systems. However, it assumes that the fluid's viscosity remains constant, meaning it does not account for shear-thinning or shear-thickening behavior - a limitation when dealing with many real-world polymer solutions [10].

To address these complexities, more advanced models have been developed. The Giesekus model, for instance, extends the capabilities of Oldroyd-B by incorporating shear-dependent viscosity, thereby enabling the prediction of more realistic flow behavior in strongly shear-thinning viscoelastic (STVE) fluids. Importantly, the Giesekus model also accounts for the second normal stress difference (N_2), which plays a role in secondary flow effects and becomes relevant in certain channel geometries or at higher concentrations [12].

Another widely used framework is the Phan-Thien-Tanner (PTT) model, which also includes shear-thinning effects and is particularly known for its numerical stability at high Weissenberg numbers. This makes it well-suited for simulating microscale flows where elastic effects dominate. Together, these models allow researchers to tailor their simulations according to the specific rheological characteristics of the fluid being studied, enhancing the accuracy and predictive power of numerical analyses in viscoelastic microfluidics.

2.1.6 Forces Acting on Microparticles in Viscoelastic Media

The dynamics of microparticles suspended in viscoelastic fluids are governed by a complex interplay of forces that can be categorized based on their relative strength and mechanisms of action. Understanding these forces is crucial for predicting and controlling particle behavior in microfluidic systems.

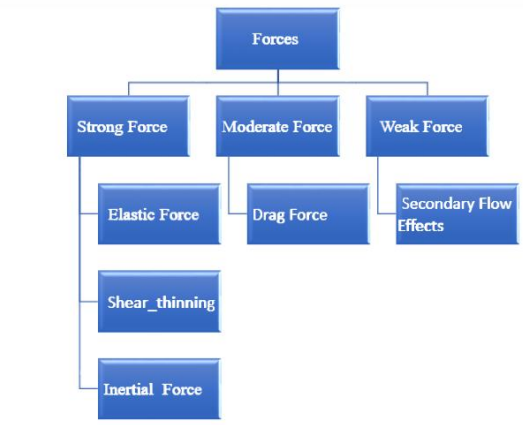

Fig. 2.1: Classification of forces in microfluidic systems.

Elastic Force (F_e)

Among the various forces acting on particles in microfluidic viscoelastic flows, the elastic force stands out as the primary mechanism responsible for lateral particle migration. This force arises due to an imbalance in the distribution of normal stresses across the surface of a suspended particle - a phenomenon that is directly linked to the first normal stress difference (N_1). According to Yuan et al., this stress imbalance - expressed as $N_1 = (\tau_{xx} - \tau_{\gamma\gamma})$ - varies across the particle surface, generating a net lateral force that pushes the particle away from regions of high shear toward areas of lower shear rate [11].

In practical terms, this means that particles suspended in a viscoelastic fluid are naturally driven toward equilibrium positions, which depend on the channel geometry and the flow profile. For example, in rectangular channels, particles often migrate toward the centerline or channel corners, where the shear rate is minimized and the elastic stress gradients create favorable migration pathways [10,11,12]. This migration occurs passively, without the need for external fields or complex device structures, making viscoelastic focusing an attractive strategy for applications such as cell sorting, bioparticle concentration, and label-free diagnostics.

The strength and direction of the elastic force depend on several factors, including polymer concentration, particle size, and flow rate, all of which influence the magnitude of N_1 and the degree of asymmetry in stress distribution. As such, understanding and harnessing this elastic force is central to designing efficient microfluidic systems that rely on the intrinsic properties of the fluid for controlled particle manipulation.

Shear-Thinning Induced Lift Force (F_{ST})

In the context of strongly shear-thinning viscoelastic (STVE) fluids, particle migration becomes more complex due to the emergence of an additional lift force - one that arises not from elasticity, but from gradients in viscosity across the particle surface. As these fluids flow, regions near the channel walls typically experience higher shear rates, leading to localized drops in viscosity. This uneven viscosity distribution creates a viscosity-induced lift force that tends to push particles toward the channel walls [10].

This force often acts in opposition to the elastic lift force, which usually drives particles toward regions of lower shear, such as the centerline. As a result, in STVE fluids, the net migration of

a particle depends on the balance between elastic and shear-thinning-induced forces. Under certain conditions - especially at moderate flow rates and higher polymer concentrations - the shear-thinning effect can dominate, leading to wall-directed migration.

Understanding this competing dynamic is critical in applications where precise particle positioning is essential. By tuning the fluid rheology and flow parameters, researchers can exploit or suppress this force to steer particles toward desired equilibrium positions, allowing for more nuanced control in microfluidic platforms used for cell sorting, particle separation, and diagnostic assays.

Inertial Forces

In microfluidic systems, the characteristic small dimensions and low flow velocities usually result in very low Reynolds numbers ($Re \ll 1$), where viscous forces dominate and inertial effects are minimal. In this creeping flow regime, fluid motion is highly predictable and laminar, making it ideal for applications that require precise control. As a result, inertial forces are often considered negligible when designing and analyzing microfluidic devices. Specifically, in viscoelastic microfluidic studies, the particle Reynolds number - a measure of how inertia affects individual suspended particles - typically ranges between 10^{-8} and 10^{-3}, confirming that viscous and elastic forces overwhelmingly govern particle dynamics [11,12].

However, the picture begins to change as the Reynolds number increases, especially when it enters the intermediate range of 1 to 5. In this regime, inertial lift forces start to play a noticeable role, influencing particle trajectories in ways that are not observed in purely viscous flows. These lift forces, arising from velocity gradients and particle-wall interactions, can cause particles to migrate laterally toward specific equilibrium positions - even in Newtonian fluids. This shift introduces new dynamics into the system, enabling more complex and tunable particle behavior.

This moderate Reynolds number range is particularly significant for the development of elasto-inertial microfluidic platforms, where both viscoelastic and inertial forces are leveraged in tandem. Devices operating in this regime can achieve enhanced focusing efficiency, faster response times, and higher throughput, making them well-suited for clinical diagnostics, biological sample processing, and other high-performance microfluidic applications. Thus,

while inertial effects are often negligible in standard microscale flows, understanding their influence becomes essential when pushing the boundaries of microfluidic design.

Secondary (Moderate) Forces

Drag Force (F_D)

The drag force is a fundamental interaction that arises whenever there is a velocity difference between a particle and the surrounding fluid. As the fluid flows around the particle, this relative motion creates a resistive force - commonly known as drag - that acts in the direction opposite to the particle's movement. This force is always present, regardless of the fluid type or flow regime, and plays an important role in determining how quickly a particle can respond to changes in the flow field [11].

However, in the context of low Reynolds number viscoelastic microflows, the influence of drag on lateral particle migration is generally secondary compared to the much more dominant elastic lift forces. While drag can affect the speed and stability of a particle's movement, it does not directly determine its migration direction or focusing position. Instead, it serves more as a damping force, modulating how rapidly a particle reaches its equilibrium location under the influence of other forces like elasticity, shear gradients, or inertial effects.

Understanding drag is still important, especially in transient flows or during the initial stages of particle entry into a microchannel, where velocity mismatches can be more pronounced. But in most viscoelastic systems operating at low Reynolds numbers, drag is a background actor, ensuring smooth particle motion while elasticity leads the way in shaping migration patterns.

Weak Forces

Secondary Flow Effects

While elastic and drag forces play primary roles in particle migration, certain weaker forces can also influence flow behavior - particularly in specific geometries or under finely tuned conditions. One such effect arises from the second normal stress difference (N_2), a lesser-known but still meaningful aspect of viscoelastic stress distribution. In microchannels with non-circular cross-sections - such as rectangular, triangular, or asymmetrical geometries - this

N_2 component can give rise to secondary flows, which occur perpendicular to the primary flow direction [10].

These secondary flows, although typically subtle, can impact particle migration patterns, especially for smaller particles that are more sensitive to local flow disturbances. Unlike larger particles, which may be governed by dominant elastic lift forces, smaller particles can experience noticeable deviations under the influence of these transverse flow components. However, in many practical cases - particularly when using dilute PEO solutions - the magnitude of N_2 is relatively small, and its effects are often negligible compared to the much stronger influence of the first normal stress difference (N_1) [11]. Nevertheless, in finely tuned systems or when extreme precision is required, these weak forces should not be entirely dismissed.

2.1.7 Dimensionless Numbers in Viscoelastic Flow

To fully understand and predict particle behavior in viscoelastic microflows, it is essential to rely on dimensionless numbers. These parameters help characterize the relative importance of different physical effects and offer valuable insight into the dominant mechanisms in a given system.

Weissenberg Number (Wi)

Among the most critical of these is the Weissenberg number (Wi), which quantifies the relative strength of elastic forces in comparison to viscous forces. It is defined as the product of the fluid's relaxation time and the characteristic shear rate. This number serves as a key indicator of how significantly elasticity will influence the flow. When $Wi \ll 1$, the fluid behaves much like a Newtonian fluid, with viscous forces dominating. When $Wi \gg 1$, the system enters an elastic-dominated regime, where polymeric stresses have a strong influence on particle migration and flow characteristics.

In microfluidic applications, the Weissenberg number can span a remarkably wide range - from as low as 0.01 to values exceeding 6000, depending on factors such as polymer concentration, molecular weight, channel geometry, and flow rate [10,12]. This wide variability makes Wi an indispensable parameter for tailoring fluid performance in different devices, allowing

researchers to design systems that either maximize or minimize viscoelastic effects, depending on the intended application.

Reynolds Number (Re)

The Reynolds number is a fundamental dimensionless quantity that captures the balance between inertial and viscous forces in a fluid flow. It is defined as:

$$\mathrm{Re}=\frac{\rho \mathrm{UL}}{\mu}$$

where ρ is the fluid density, U is a characteristic flow velocity, L is the characteristic length (such as channel height or width), and μ is the dynamic viscosity of the fluid. This ratio helps determine the nature of the flow: whether it is laminar and stable (dominated by viscous forces), or turbulent and unstable (dominated by inertia).

In the realm of viscoelastic microfluidics, maintaining a low Reynolds number - typically Re < 1 - is essential to ensure viscous-dominated laminar flow, which enables precise control over particle dynamics and flow symmetry [12]. Under these conditions, the influence of inertial effects is minimal, allowing researchers to focus on the more subtle interactions such as elastic forces and shear gradients.

To further understand how inertia affects individual particles suspended in flow, the particle Reynolds number ($\mathrm{Re_p}$) is used. It is defined as:

$$\mathrm{Re_p}=\frac{\rho \mathrm{UpD}}{\eta}$$

Here, U_p is the particle velocity, D is the particle diameter, and η represents the dynamic viscosity (sometimes interchanged with μ). This formulation quantifies the degree to which inertia influences a particle's motion relative to the surrounding fluid.

In most microfluidic systems involving dilute polymer solutions and micron-scale particles, $\mathrm{Re_p}$ values are extremely low — often ranging from 10^{-8} to 10^{-3} — indicating that viscous and elastic forces overwhelmingly dominate, with inertia playing only a minor role [11]. Nevertheless, in some intermediate Reynolds number regimes, these inertial effects can become relevant and understanding Re and $\mathrm{Re_p}$ is crucial for accurately modeling flow behavior and designing advanced particle manipulation systems.

Blockage Ratio (β)

Another important dimensionless parameter in viscoelastic microfluidics is the blockage ratio (β), which plays a key role in determining how particles behave as they travel through microchannels. It is defined as the ratio of the particle diameter (D) to the hydraulic diameter of the channel (Dh):

$$\beta = \frac{D}{Dh}$$

This ratio essentially quantifies how much of the channel cross-section is occupied by a particle, and it strongly influences both the magnitude of forces acting on the particle and the efficiency of particle migration.

In general, a larger blockage ratio results in a stronger elastic lift force acting on the particle. This is because larger particles experience greater variations in the viscoelastic stress field across their surface, particularly in regions of steep shear gradients. As a result, the elastic forces responsible for lateral migration become more pronounced, allowing the particle to move more rapidly toward its equilibrium position [10,12].

However, increasing the blockage ratio also introduces greater sensitivity to flow disturbances and can affect the stability of the particle's final focusing position. While larger particles may achieve faster migration, they are also more susceptible to instabilities caused by changes in flow rate, channel geometry, or polymer concentration. Therefore, selecting an optimal blockage ratio is a balancing act — one that depends on the desired speed, precision, and robustness of the focusing behavior in a given microfluidic design. Understanding and appropriately tuning β is especially critical in applications such as cell sorting, size-based separation, and single-particle analysis, where precise control over particle position is essential for achieving high resolution and throughput.

2.1.8 Migration Regimes and Flow Phenomena

Recent research has identified multiple distinct migration regimes for particles in viscoelastic flows, depending on the interplay between the dimensionless parameters discussed above. Hazra et al. identified five primary regimes: original streamline (OS), bimodal (BM), center migration (CM), defocusing (DF), and wall migration (WM) [12]. These regimes emerge from

the synergistic effects of viscoelastic lift forces and shear-thinning induced forces, with their occurrence dependent on the STVE parameter (α) and average strain rate ($\dot{\gamma}$). The transition between these regimes provides valuable insights into the underlying physics and offers opportunities for controlled particle manipulation in microfluidic devices. The ability to predict and control these transitions represents a significant advancement in the field of viscoelastic microfluidics.

2.1.9 Passive Particle Transfer in Viscoelastic-Newtonian Interfaces

Yuan et al. (2016) conducted an experimental study to understand particle lateral migration behavior in a sample–sheath microfluidic system where fluids of different rheological properties—viscoelastic and Newtonian—co-flowed in a straight microchannel. The primary goal was to demonstrate how particles suspended in a viscoelastic fluid (PEO solution) migrate laterally into a Newtonian (DI water) sheath flow, a phenomenon not typically achievable in laminar flows without external forces or complex channel geometries.

The microchannel used was a simple straight rectangular design, and 4.8 μm polystyrene particles were suspended in various concentrations of PEO (500, 1000, and 5000 ppm). The particle-laden viscoelastic fluid was introduced alongside DI water as the sheath flow. Notably, particles consistently migrated from the viscoelastic stream to the Newtonian stream, but not in the reverse direction, confirming the directional selectivity of the migration process driven primarily by elastic lift forces [13].

The study systematically investigated the influence of channel length, flow rate ratios, and PEO concentration on particle migration. Results showed that increasing the channel length and the sheath-to-sample flow rate ratio enhanced particle migration and focusing. Among the tested concentrations, 1000 ppm PEO offered optimal performance, balancing elastic force strength and manageable viscosity. At higher concentrations (e.g., 5000 ppm), particle migration efficiency decreased due to diffusion effects and increased viscosity, which hindered lateral movement [13].

Comparative experiments with Newtonian–Newtonian and Newtonian–viscoelastic sample-sheath configurations confirmed that the lateral migration observed was unique to particles

initially suspended in a viscoelastic fluid. These findings open up possibilities for implementing simple and effective passive solution exchange techniques in microfluidic platforms, particularly for biomedical tasks like cell washing and staining, without relying on external fields or complex device structures [13].

2.1.10 Enhanced Viscoelastic Focusing via Gradual Channel Contraction.

Fan et al. (2020) proposed a novel microchannel design to enhance particle focusing in viscoelastic fluids using a passive method. The study introduced a straight microchannel with a gradually contracted geometry, which significantly improved lateral particle migration through a combination of elastic lift force, viscous drag, and Saffman lift force. This geometric configuration altered the local shear rate distribution and introduced lateral flow components, enabling particles to rapidly migrate toward the channel center [14].

The research employed both numerical simulations and experimental validation. Three different channel types were fabricated: a straight rectangular channel, a gradually contracted channel, and one with a small orifice to isolate the influence of outlet geometry. Particles of various sizes (4, 7, and 10 μm) suspended in viscoelastic fluids—1000 ppm PEO and 8 wt% PVP—were tested at flow rates ranging from 1 to 50 μL/min. Results indicated that the gradually contracted channel achieved significantly tighter focusing in much shorter lengths (~1 cm) compared to traditional straight channels (~4–10 cm), making it ideal for compact lab-on-a-chip devices [14].

Notably, the study found that fluid rheology played a critical role: the PVP solution, having a higher elastic-to-inertial force ratio, enabled more efficient focusing at lower Weissenberg numbers than the PEO solution. Particle size also influenced focusing performance, with larger particles responding more effectively to elastic and drag forces.

Overall, the study demonstrated that a carefully designed channel geometry can enhance viscoelastic particle focusing performance without external forces or complex device architecture. The findings provide a solid foundation for developing efficient, compact, and high-throughput microfluidic platforms for biomedical and diagnostic applications [14].

2.1.11 Numerical Modeling of Viscoelastic Focusing in Cavity-Structured Channel.

Wang et al. (2023) conducted a comprehensive numerical study to investigate microparticle manipulation in viscoelastic microfluidic flows using a microchannel embedded with asymmetrical triangular cavities. The motivation behind the study was to better understand particle lateral migration mechanisms in complex channel geometries, which had previously been examined experimentally but lacked in-depth theoretical interpretation [15].

A two-dimensional numerical model was developed using COMSOL Multiphysics 6.0 to simulate the viscoelastic fluid behaviour and particle dynamics. The simulations incorporated the Phan-Thien/Tanner (PTT) constitutive model to handle large Weissenberg numbers and achieve numerical stability. The study considered a range of flow rates (10–80 μL/min) and PEO polymer concentrations (500–2000 ppm) to examine their influence on flow characteristics and particle focusing [15].

The model was validated against prior experimental results and showed strong agreement. Key findings revealed that the first normal stress difference (N_1) is the primary driver of lateral particle migration, with elastic lift forces pushing particles away from the cavity side toward a stable focusing position. It was observed that higher flow rates enhanced elastic forces and improved particle focusing, while higher polymer concentrations decreased the magnitude of elastic force due to increased viscosity.

Additionally, the study evaluated the combined effects of drag, inertial lift, and elastic forces, offering a detailed explanation of how geometry and fluid rheology interact to guide particle behaviour. Grid independence analysis and flow field validation further strengthened the model's reliability.

Overall, the work by Wang et al. provides a validated numerical framework to analyse particle migration in non-standard microchannel geometries and serves as a reference for optimizing passive viscoelastic microfluidic systems used in biomedical and lab-on-a-chip applications.

2.1.12 Selective Lateral Particle Migration in Viscoelastic–Newtonian Co-flows

Yuan et al. (2016) explored a unique form of particle manipulation by leveraging the distinct rheological properties of viscoelastic and Newtonian fluids in a sample–sheath flow configuration. The central objective was to achieve passive lateral migration of particles across streamlines — a task typically requiring complex channel designs or external force fields. In

their approach, 4.8 μm fluorescent polystyrene particles were suspended in a polyethylene oxide (PEO) viscoelastic solution and introduced alongside a Newtonian sheath flow of deionized water in a straight microchannel. Remarkably, the particles migrated from the viscoelastic stream into the Newtonian stream, but not in the reverse direction, indicating a directional migration behaviour driven by elastic forces [16].

Through systematic experimentation, the authors evaluated the impact of channel length, flow rate ratios, and polymer concentration on migration performance. It was observed that increasing the sheath-to-sample flow rate ratio resulted in a more confined viscoelastic stream and improved particle focusing. Similarly, longer channels allowed more time for particles to traverse the interface, resulting in tighter focusing downstream. Among the tested concentrations, 1000 ppm PEO provided the most effective balance between elastic force strength and manageable viscosity, facilitating efficient particle transfer. In contrast, at higher concentrations (e.g., 5000 ppm), increased fluid viscosity and enhanced diffusion disrupted migration and focusing performance [16].

To validate the phenomenon, the researchers conducted comparative experiments using other fluid pairings, such as Newtonian–Newtonian and Newtonian–viscoelastic flows. In both cases, lateral migration did not occur, confirming that elasticity must be present in the particle's initial medium for migration to take place. This reinforces the idea that the elastic lift force, generated by first normal stress difference (N_1) within the viscoelastic stream, is the dominant mechanism behind the migration.

Furthermore, their findings revealed that after particles exited the viscoelastic region, they continued to migrate laterally for a short distance within the Newtonian flow. This was attributed to the inertial carry-over of motion, although the particle Reynolds number was very low ($Rp \approx 0.03$), confirming that the contribution from inertial lift forces was negligible [16].

2.1.13 Migration Dynamics of Droplets in Shear-Thinning Viscoelastic Media

In an effort to better understand droplet transport in rheologically complex fluids, Hazra et al. (2020) carried out a detailed experimental and analytical investigation into the lateral migration behaviour of Newtonian and viscoelastic droplets in shear-thinning viscoelastic (STVE) microflows. While most prior work focused on particle migration in either purely viscoelastic

or Newtonian fluids, this study sheds light on the nuanced dynamics introduced when shear-thinning and elasticity coexist in the medium [17].

The experiments were conducted using polymeric STVE liquids-including polyethylene oxide (PEO), polyacrylic acid (PAA), and polyacrylamide (PAM)-with varying molecular weights and concentrations. PDMS and castor oil droplets of different sizes were generated in T-junction and flow-focusing microchannels, allowing observation of droplet behavior under a wide range of flow conditions. The system was maintained at low Reynolds numbers ($Re < 1$), where inertial effects are minimal, and elasticity dominates, with Weissenberg numbers (Wi) ranging from 0.01 to 7.4. This experimental regime closely mimics the physiological conditions relevant to biological fluid applications [17].

A key observation was that smaller droplets (blockage ratio $\beta \leq 0.2$) tend to migrate toward the channel center, while larger droplets ($\beta \geq 0.28$) follow their original streamlines. This size-dependent behavior was attributed to a delicate balance of multiple forces: the non-inertial lift force (FNIL), the viscoelastic lift due to the continuous phase (FVM), and-when applicable-the discrete-phase viscoelastic lift (FVD). Interestingly, the study found that existing models based on these forces alone could not explain the behavior of larger droplets, particularly their resistance to centerward migration in STVE media. To address this, the authors introduced a novel concept: the shear-thinning-induced lift force (FSM), which acts toward the channel wall and counterbalances other migration-inducing forces [17].

Another key takeaway was the independence of migration behavior from interfacial tension (IFT) and the dominant role of fluid rheology and droplet deformability. The study also confirmed that internal droplet properties, like viscosity and elasticity ratios (k and ξ), significantly impact migration velocity and trajectory, especially for smaller droplets.

Overall, this work not only introduced a new force mechanism (FSM) into the existing viscoelastic microfluidic paradigm but also provided a validated model that can be extended to both rigid and deformable particles in diverse shear-thinning environments. The findings are particularly relevant for size-based droplet sorting, single-cell encapsulation, and biomedical assays, where rheology-driven migration can be leveraged for passive, label-free microfluidic separation strategies.

2.1.12 Summary

The literature reveals that viscoelastic fluids present a rich and complex medium for microparticle manipulation, offering unique advantages over conventional Newtonian fluid systems. The elastic forces arising from normal stress differences provide the primary mechanism for particle migration, while shear-thinning effects introduce additional complexity that can be exploited for enhanced control. The interplay between various dimensionless numbers determines the flow regime and particle behavior, enabling precise manipulation of particles ranging from submicron to tens of microns in size.

Understanding these fundamental principles is essential for advancing applications in cell sorting, particle separation, and biomedical diagnostics. The continued development of theoretical models and experimental techniques will further enhance our ability to harness the unique properties of viscoelastic fluids for practical microfluidic applications.

2.2 Literature Gap

Despite significant advancements in the field of viscoelastic microfluidics, several gaps remain unaddressed in current research. Most existing studies focus on standard microchannel geometries—typically straight channels or simple expansions—when evaluating particle migration in viscoelastic fluids. However, the influence of more intricate and varied cavity designs, such as asymmetric or periodic well patterns, on particle focusing has not been thoroughly explored.

Furthermore, while many studies report experimental findings or rely on idealized assumptions, limited attention has been given to systematically evaluating the cumulative effect of channel geometry, the number of geometric features (e.g., wells), and varying polymer concentrations on particle deviation in a unified simulation framework. Also, the majority of research targets binary particle separation, with less emphasis on fine-tuning geometric structures for maximizing focusing performance or minimizing pressure drop in passive systems. There is a need for a deeper understanding of how localized flow disturbances—introduced by specific geometric modifications—interact with viscoelastic properties to influence particle migration. Addressing this knowledge gap can enhance the design of more efficient microfluidic devices for practical applications, especially in biomedical diagnostics and lab-on-a-chip systems.

2.3 Objectives of the Present Work

The primary aim of this study is to investigate the role of microchannel geometry in influencing microparticle behavior in viscoelastic flows using a simulation-based approach. The specific objectives are as follows:

1. **Model Validation:** To validate a viscoelastic particle migration model by replicating results from a previously published, experimentally verified study, thereby establishing the reliability of the simulation framework.
2. **Geometric Variation Analysis**: To systematically study the effects of various well geometries—such as symmetric and asymmetric rectangular, triangular, and curved cavities—on particle focusing and lateral deviation.
3. **Effect of Polymer Concentration**: To evaluate how changes in polymer concentration (PEO at 500 ppm and 1000 ppm) impact viscoelastic lift forces and particle migration patterns across different channel designs.
4. **Influence of Well Count**: To analyze how increasing the number of embedded wells affects the cumulative particle deviation and to determine if there exists a saturation point beyond which further wells offer diminishing returns.
5. **Pressure Drop Evaluation**: To compare the pressure drops associated with different channel geometries and identify configurations that offer a balance between effective particle manipulation and operational efficiency

Chapter 3

Methodology

3.1 Schematics of channel Geometry

The schematic figure of the microchannels used in this study is shown in Figure 1. The microchannel domain is a straight channel with a cross-section of 100 µm × 40 µm (width × height) with a range of additional cavities.

This study covers 4 distinct cavity designs covering both symmetric and asymmetric patterns.

1. Single side Rectangle with height of 450 µm and length of 900 µm.
2. Single side Curved well with radius of 450 µm taken from the channel center axis.
3. Both side Rectangle with height of 450 µm and length of 900 µm.
4. Both side Isosceles triangle with base length of 900 µm and height of 450 µm.

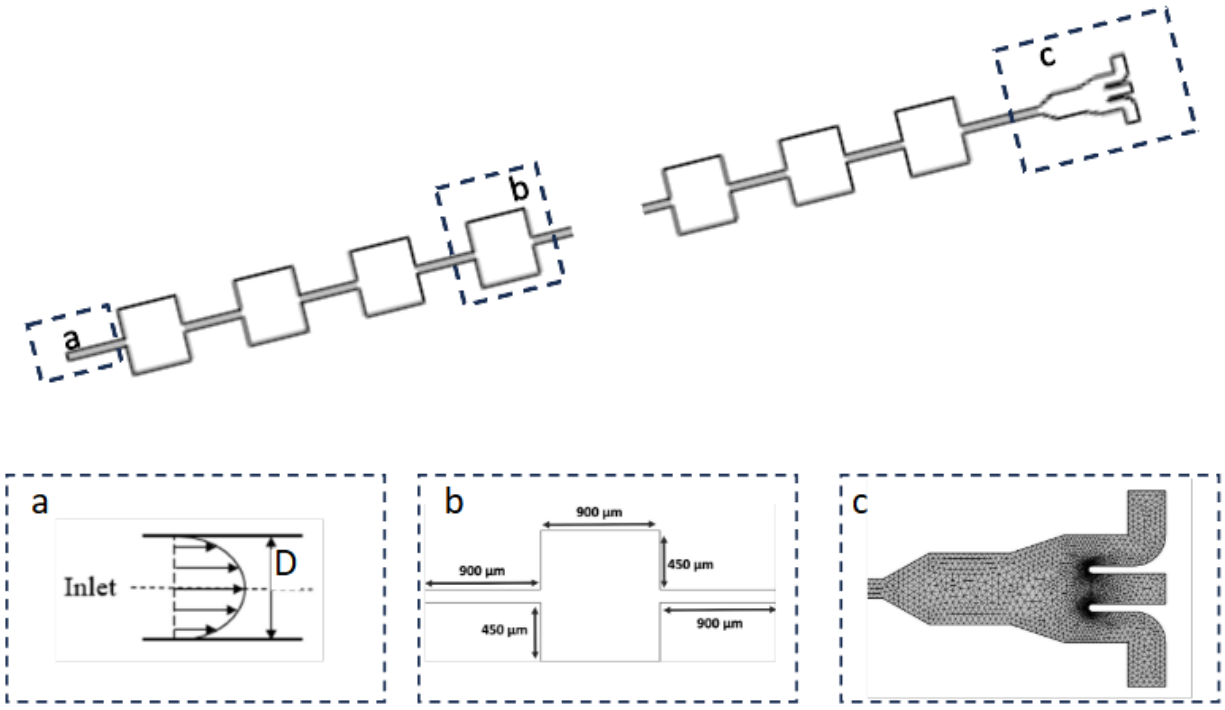

Figure 3.1.1: The Schematics of the microchannel with array of symmetric wells in the form of a) velocity distribution at the inlet of the geometry b) dimensions of the symmetric rectangular well c) meshing at the outlet of the channel.

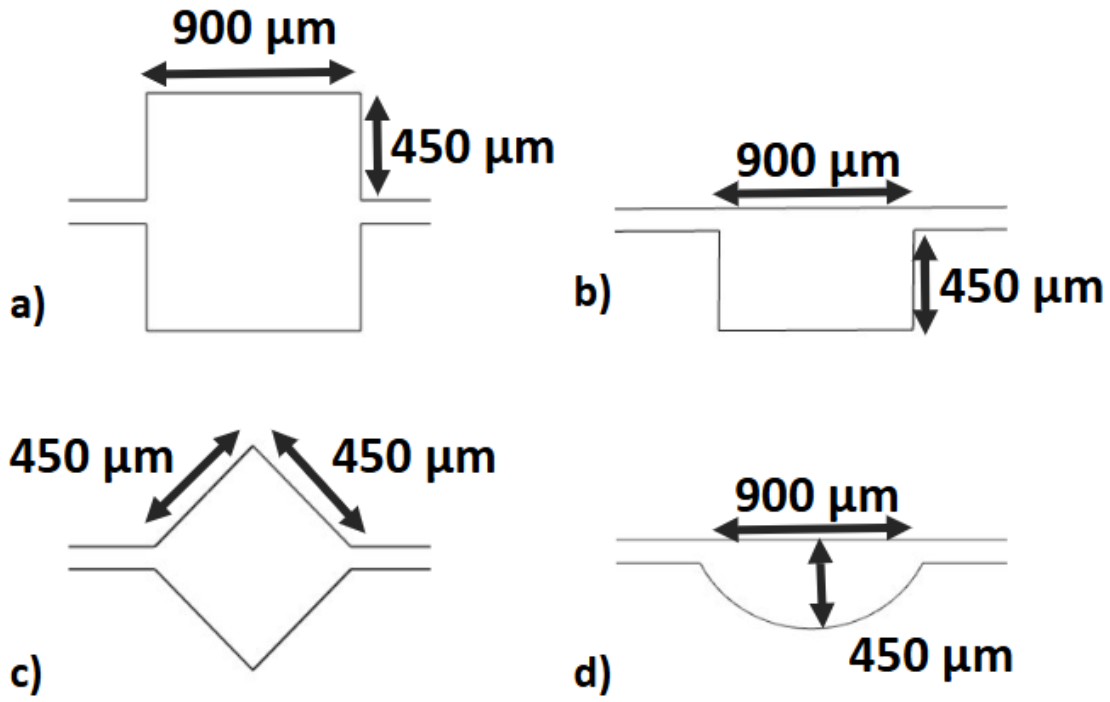

Figure 3.1.2: Variation in well shapes, a) symmetric channel with rectangular wells on each side, b) asymmetric channel with rectangular wells, c) symmetric channel with triangular wells, d) asymmetric channel with curved wells.

Along with this variation, a range of wells is also taken in consideration for symmetric channels Ranging from 11 to 36 with increments of 5The microchannel design includes 26 cavity structures, with each pair of adjacent cavities spaced 900 µm apart, resulting in a total channel length of 48 mm. Given that the channel height is significantly smaller than both its length and width (H << L and H << W), the problem was simplified to a two-dimensional model for computational efficiency.

The simulation was carried out using COMSOL Multiphysics 6.0, where the fluid behavior was first analyzed under a stationary study using the viscoelastic fluid module. Because the Reynolds number across the domain was well below 2000, the flow was assumed to be steady and laminar. The steady-state fluid field results were then used as inputs for the particle tracing module, allowing for the tracking of microparticle positions and velocities over time as they migrated through the channel.

The dynamic viscosity of the PEO (polyethylene oxide) solutions was estimated based on concentration, with values of approximately 2×10^{-3} Pa·s for 500 ppm, 3×10^{-3} Pa·s for 1000 ppm, and 5×10^{-3} Pa·s for 2000 ppm [15]. Corresponding relaxation times were calculated as 9.1 ms, 12.4 ms, and 19.5 ms for the 500 ppm, 1000 ppm, and 2000 ppm solutions, respectively. [15]

For the simulation setup, a fully developed velocity profile was applied at the inlet, while the outlet pressure was set to 0 Pa to ensure proper flow control. The computational geometry was discretized using a refined mesh, with locally dense elements near the outlets to capture flow behavior accurately, as illustrated in Figure 3.1.1(c).

3.2 Forces involved.

The viscoelastic behavior in the fluid arises from the presence of dissolved polymer chains. When these viscoelastic fluids are subjected to shear flow within a confined channel, the polymer chains are stretched along the primary flow direction, disrupting their equilibrium state and causing an anisotropic stress distribution throughout the fluid.

In the presence of suspended microparticles, this uneven stress distribution results in a difference in normal stress on either side of each particle. This imbalance generates lateral elastic forces that drive the particles across streamlines, typically toward regions of lower shear rate. As a result, microparticles in viscoelastic fluids tend to migrate toward specific equilibrium positions—a phenomenon known as viscoelastic focusing.

To analyze this behavior quantitatively, the stress distribution around a fluid micro-element is commonly described using two normal stress differences: the first normal stress difference $N_1 = \tau_{xx} - \tau_{yy}$, and the second normal stress difference $N_2 = \tau_{yy} - \tau_{zz}$. In most polymer solutions, including PEO-based fluids, N_1 is positive and tends to decrease with increasing polymer concentration, whereas N_2 is typically negative and increases in magnitude with concentration. However, for dilute PEO solutions, N_2 is significantly smaller than N_1 and can often be neglected in practical analysis.

Therefore, the lateral elastic force F_E acting on the microparticles is primarily governed by N_1 , and it plays a key role in directing particles toward stable positions within the microchannel [18].:

$$F_E \sim a^3 \nabla N_1 = a^3 \left(\nabla \tau_{xx} - \nabla \tau_{yy} \right)$$

The viscoelastic strength of a fluid can be quantitatively described using the Weissenberg number (Wi), a dimensionless parameter that represents the ratio of elastic to viscous effects in a flow [1]. It is defined as:

$$Wi = \frac{\lambda}{t_f} = \lambda \dot{\gamma} = \frac{2\lambda U_m}{w} = \frac{2\lambda Q}{hw^2}$$

Here, λ is the relaxation time of the fluid, U_m is the average flow velocity, Q is the volumetric flow rate, and w and h are the width and height of the channel, respectively. The characteristic time t_f is inversely related to the average shear rate $\dot{\gamma}$, which can be approximated as $2U_m/w$ or $2Q/(hw^2)$ for rectangular channels. A higher Weissenberg number indicates stronger elastic effects relative to viscous forces.

On the other hand, the inertial effects in the fluid are captured by the Reynolds number (Re), another dimensionless quantity used to characterize the flow regime [19]. It is given by:

$$Re = \frac{\rho U_m D_h}{\mu} = \frac{2\rho Q}{\mu(w + h)}$$

where ρ is the density of the fluid, U_m is the flow rate of the fluid, D_h is the hydraulic diameter of the flow channel, μ is the dynamic viscosity. Dh of the flow channel is related to the type of flow channel cross-section; for a rectangular cross-section flow channel commonly used in microfluidic control, the value of the hydraulic diameter can be estimated as $D_h = 2wh/(w + h)$, in which w and h are the width and height of the flow channel cross-section, respectively

The vector of wall lift force and shear-gradient lift force are combined to be the net inertial lift force, which is used through a available module in COMSOL. It is governed by the equations

$$F_L = \rho \frac{r_p^4}{D^2} \beta\left(\beta G_1(s) + \gamma G_2(s)\right) n$$

$$\beta = \left| D(n \cdot \nabla) u_{\parallel} \right|$$

$$\gamma = \left| \frac{D^2}{2} ((n \cdot \nabla)^{2u_{\parallel}}) \right|$$

$$u_{\parallel} = (I - n \otimes n) u$$

s is the normalized distance to the first parallel boundary

n is the unit vector from the nearest point on the first parallel boundary

D is the distance between the walls

A drag force arises when an object moves through a fluid or when the fluid flows past an object, due to a velocity difference between the particle and the fluid [16], which can be estimated by:

$$F_D = 3\pi\mu a\left(v_f - v_p\right)$$

where v_f and v_p are the velocities of the fluid element and particles, respectively

3.3 Governing Equations

Assuming that the viscoelastic fluid behaves as an incompressible and continuous medium, its motion can be described using two fundamental governing equations: the continuity equation, which ensures mass conservation, and the momentum conservation equation, which accounts for the balance of forces acting within the fluid. These equations form the basis of the control equations used to simulate viscoelastic fluid flow in microfluidic environments [15,20].

$$\rho \nabla \cdot u = 0$$

$$\rho(u \cdot \nabla)u = \nabla \cdot [-pI + K + T_e]$$

$$\lambda \nabla T_{em} + \exp\left(\frac{\lambda \epsilon}{\mu_p} tr(T_{em})\right) T_{em} = 2\mu_{pD}$$

$$D = \frac{1}{2}(\nabla u + (\nabla u)^T)$$

$$\nabla T_{em} = (u \cdot \nabla) T_{em} - \nabla u \cdot T_{em} - T_{em} \cdot (\nabla u)^T$$

where $T_e = \sum_m T_{em}$ is the viscoelastic component of the stress tensor, which can be described by a different constitutive model [21,22,23]. In this study, particular emphasis is placed on the first normal stress difference, as it plays a significant role in shaping the flow field within viscoelastic fluids. To accurately capture the relationship between this stress difference and flows with high Weissenberg numbers, the Oldroyd-B model was modified by introducing an additional parameter ε, resulting in the Phan-Thien/Tanner (PTT) model. This modification improves the model's numerical stability and ensures convergence under high elasticity conditions [20]. In the governing equations, u represents the fluid velocity vector, p denotes the pressure field, and I is the identity tensor, which appears in the formulation of the stress and deformation relationships., $K = 2u_sD$ is the Newtonian component of the stress tensor, us and up are solvent viscosity and polymer viscosity, which sum to u, and the retardation factor β is defined as $\beta = u_s/(u_s + u_p)$. D is the strain velocity tensor, ε is the rheological parameter of the PPT model [20].

3.4 Boundary Conditions

At the inlet of the microchannel, a fully developed flow condition is applied, characterized by a parabolic velocity profile that reflects the steady-state distribution of velocity typically observed in laminar flow through a confined channel:

$$v_y = 0, \quad v_x \text{ is parabolic profile}$$

In channel flow, symmetry exists along the centerline, which implies that both the normal velocity component and the tangential shear stress vanish at this boundary. This condition is a direct result of the flow's symmetrical nature about the centerline:

$$\frac{\partial v_x}{\partial y} = 0, \quad v_y = 0, \quad \sigma_{xy} = 0$$

Since the velocity profile and stress tensor components play a crucial role in accurately resolving the flow behavior—especially when these quantities stabilize at a sufficient distance from the inlet—the initial stress tensor is explicitly defined at the channel entrance to ensure consistent and realistic simulation results:

$$\sigma^*_{vxx} = \sigma^*_{vxy} = \sigma^*_{vyy} = 0$$

The model applies a no-slip boundary condition along the channel walls, ensuring that the fluid velocity relative to the wall is zero. Additionally, a pressure outlet condition is implemented at all three outlet boundaries to represent fully developed flow, allowing the fluid to exit the domain smoothly without introducing backflow or artificial constraints:

$$[-pI + K + T_e]n = -p_{0n}, \quad p_0 = 0$$

To simulate the behavior of viscoelastic fluids, the process begins with a stationary solution, which provides a stable initial condition for solving the problem. The simulations are conducted using COMSOL Multiphysics 6.0, which employs the finite element method (FEM) to numerically solve the governing equations. To ensure numerical stability and convergence, particularly at high Weissenberg numbers, the Phan-Thien/Tanner (PTT) model is implemented.

Among the available solvers, the PARDISO solver is selected over MUMPS due to its better performance in this context. The solver settings are configured with relative and absolute tolerances of 10^{-5} and 10^{-6}, respectively, and a time step of 0.001 seconds. Convergence is achieved by iteratively adjusting the residual values until they drop below the predefined tolerance thresholds.

The stationary fluid simulation is executed for approximately 120 seconds, yielding a steady-state flow field. This result is then used as the initial condition for the particle tracking simulation, which predicts the migration paths of suspended particles over time. Each operating condition is simulated for about 20 minutes to ensure sufficient data resolution for analysis.

3.5 Grid Independence Test:

Table 3.5 Mesh types and corresponding number of elements used in numerical simulations

Mesh type	Number of Elements
Normal	18795
Fine	29448
Finer	101147

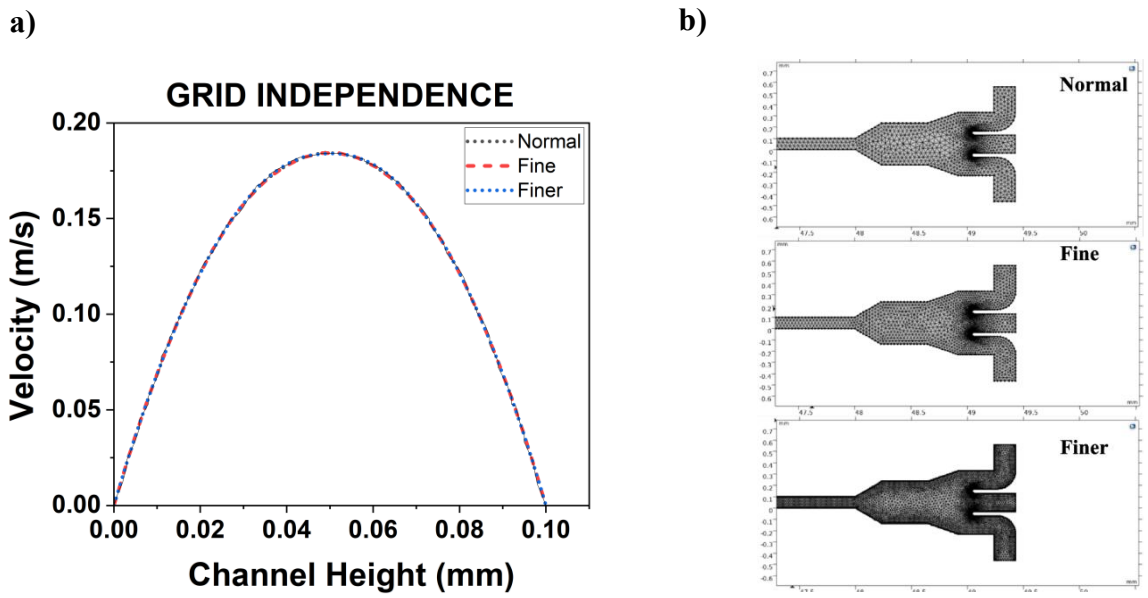

Figure 3.5: Grid independence analysis with a) velocity profiles at different mesh densities and b) nature of channel outlet at different mesh densities.

The grid independence test was carried out to ensure that the simulation results are not influenced by the choice of mesh density but instead reflect the true physics of the flow. Three different mesh types were tested: normal (18,795 elements), fine (29,448 elements), and finer (101,147 elements). By comparing the velocity profiles across the channel height for each mesh, it was observed that all three mesh densities produced nearly identical results, as shown by the overlapping curves in the velocity plot. This close agreement indicates that further refining the mesh does not significantly change the solution, confirming that the simulation is grid independent. As a result, the Fine mesh was selected for subsequent analysis, as it offers

a good balance between computational efficiency and accuracy. This approach ensures that the numerical findings are robust and reliable, providing confidence in the simulation outcomes for the viscoelastic microchannel study

3.6 Extensibility comparison

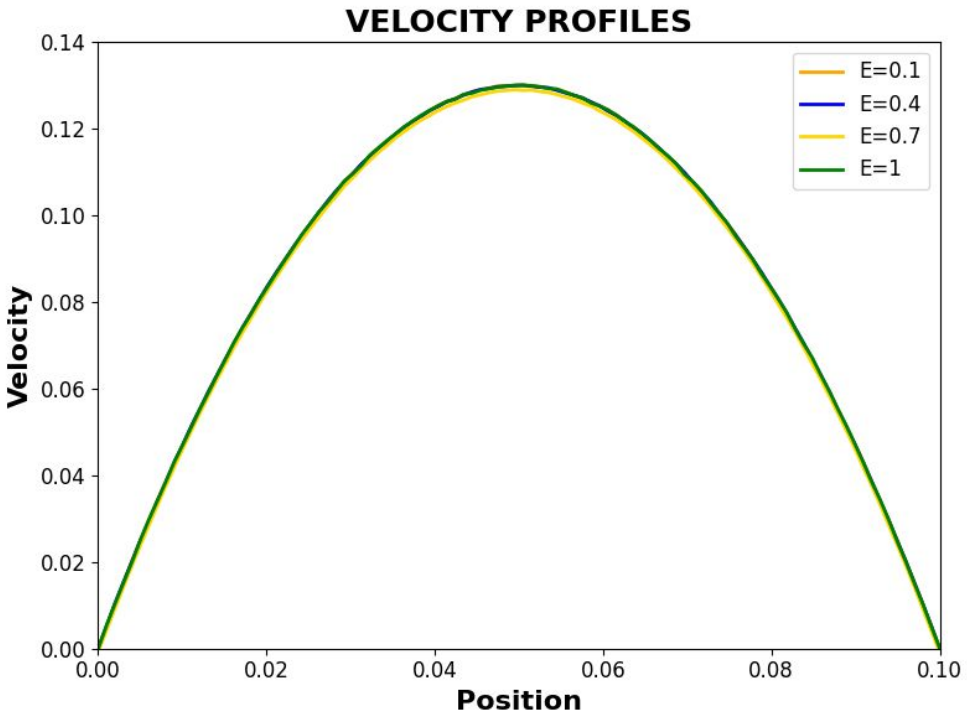

Figure 3.6: Velocity profiles at the microchannel inlet for different fluid extensibility values at a flow rate of 20 μL/min.

The figure presents velocity profiles at the inlet of a microchannel for a flow rate of 20 μL/min, comparing the effects of different fluid extensibility values (E = 0.1, 0.4, 0.7, 1). The profiles for each extensibility value overlap almost perfectly, indicating that changes in the extensibility parameter have negligible influence on the velocity distribution across the channel at this flow rate. This result demonstrates that, under these conditions, the fluid's extensibility does not significantly affect the inlet velocity profile. As a result, a fixed extensibility value of 0.5 is chosen for all subsequent simulations to simplify the analysis without compromising accuracy.

3.7 Validation

To ensure the accuracy and reliability of the simulation model, the same geometrical configuration used by **Tiao Wang (2023)** was replicated [15]. This model was then tested to see if it could reproduce the experimental observations reported in Wang's study.

The validation process involved simulating particle flow under two different flow rates—30 µl/min and 40 µl/min—with a polyethylene oxide (PEO) concentration of 1000 ppm. The simulation outcomes were then compared with the experimental data.

- At 30 µL/min, the simulation showed that the particle stream split at the outlet, with particles exiting through two separate channels. This behaviour matched the experimental observations, confirming the model's accuracy at this flow rate.
- At 40 µl/min, the simulation revealed that the particle stream converged and exited through a single outlet, again in agreement with the experimental results.

This comparison, illustrated in **Figure 3.7**, demonstrates that the simulation model can reliably replicate the behaviour of particle streams under varying flow conditions, thereby validating its use for further analysis.

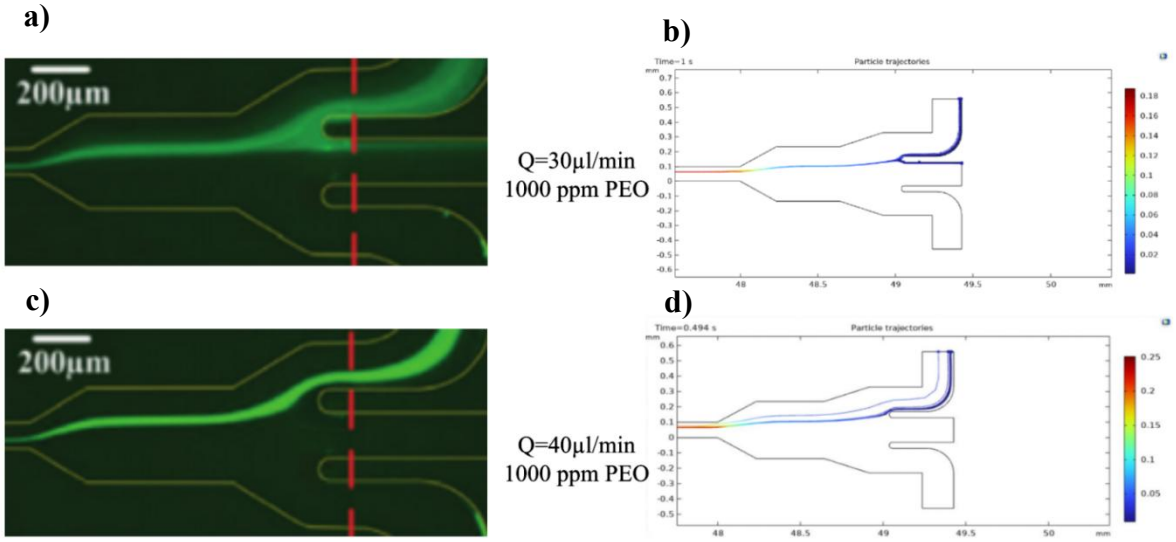

Figure 3.7: Comparison between a) experimental and b) simulation results for a flow rate of 30 µl/min and c) experimental and d) simulation results for a flow rate of 40 µl/min at 1000 ppm PEO concentration [15].

3.8 Inverted Geometry.

To further validate the robustness and generalizability of the simulation model, the same flow simulation was conducted using an inverted version of the original geometry. The goal was to determine whether the model could still accurately predict particle behavior under altered structural conditions. The results from the inverted geometry closely mirrored those from the original configuration. This consistency suggests that the deviation of suspended particles is not solely dependent on the geometry's orientation but is also significantly influenced by shear-induced lift forces. These forces arise due to velocity gradients created by the presence of microstructural features such as wells.

To explore this phenomenon further, the study examined a variety of well geometries, including:

- Rectangular wells
- Curved wells
- Double-sided triangular wells
- Double-sided rectangular wells

Each of these geometries was analyzed to observe how their unique shapes affect the behavior and deviation of suspended particles in the flow. The simulation was conducted at a flow rate of 40 µl/min using a 500 ppm PEO (polyethylene oxide) solution, providing a controlled environment to assess the influence of geometry on particle dynamics.

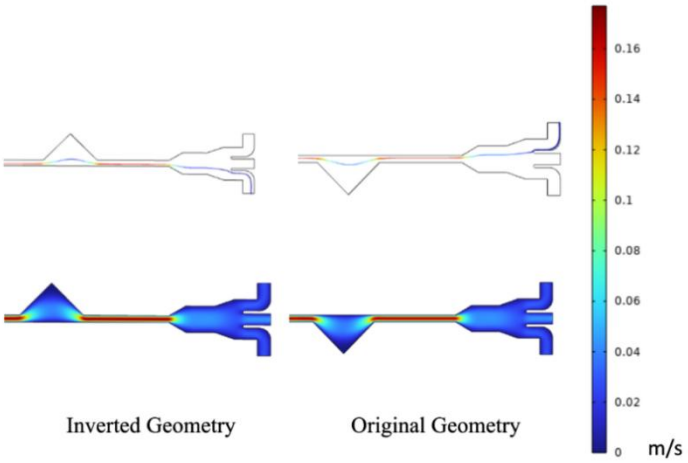

Figure 3.8: Comparison between particle deviation at original profile[15] and inverted profiles at a flowrate of 40 µl/min at 500 ppm PEO solution.

Chapter 4

Results and Discussion

In this study, we explore the effects of geometrical variation on the flow of micro particles suspended in a Viscoelastic medium. Building on the previous work by Wang et al. (2023), the channel geometry, more specifically, the shape of wells, had been altered, ranging from symmetric channels with both sides rectangular and both sides triangular wells to asymmetric channels with rectangular and curved wells. To study the effect of geometry and the viscoelastic lift force on the suspended particles, all particles are released from the center of the straight channel with a frequency of 1 micro particle per 0.001 sec. This study is restricted to a flow rate of 40 L/min due to constraints provided by the simulation model. Therefore, the fluid is fed at 3 different flow rates ranging from 20-40 µL/min with a step of 10 µL/min. The particle size is fixed at 4.8 µm to mimic the behavior of a red blood cell.

4.1 Flow development across different well shapes.

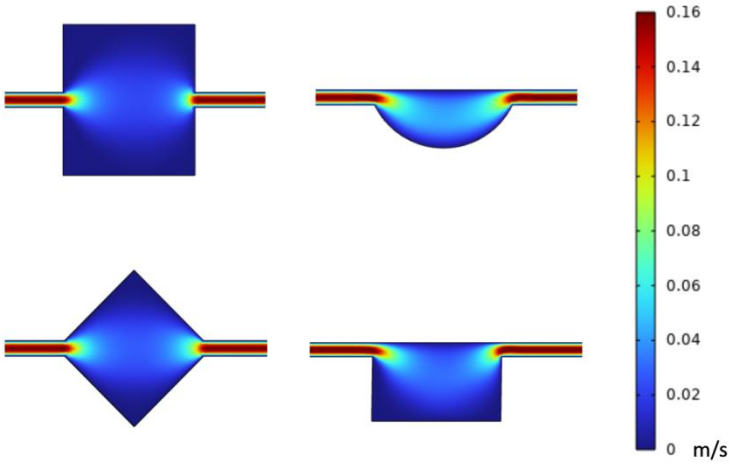

Figure 4.1: Velocity contour for all channel geometries at 30 µL/min.

The figure presents a comparison of velocity contours for different well shapes embedded within a microchannel, illustrating how the geometry of these wells influences the fluid dynamics and particle behavior in such confined environments. Across all the geometries, the highest velocities are consistently observed at the channel inlets and outlets, as indicated by the

red and yellow regions on the contour plots, while the velocity drops markedly within the well regions themselves, especially in areas where the channel expands and the fluid has more space to spread out.

Rectangular wells and both side rectangular wells tend to generate broad zones of slow-moving fluid in their centers, and the velocity profile recovers rapidly as the fluid exits the well and moves back into the narrower channel, resulting in a sharp transition between low and high velocity regions. In contrast, semi-circular wells create deeper, more pronounced zones of low velocity at their bases, while both side square wells, due to their sharp corners, produce localized pockets of very low velocity in those corners, leading to more complex flow patterns and recirculation zones.Low shear rate zones, which are regions where the velocity gradient is minimal, are predominantly found in the center and corners of the wells, particularly in larger or more rounded cavities1. These zones are significant in viscoelastic microfluidics because particles suspended in the fluid tend to migrate and accumulate there, driven by elastic lift forces that are maximized in areas of low shear. This phenomenon is especially beneficial for applications such as particle focusing and separation, where precise control over particle positioning is require.

4.2 Deviation of particles at different flow rates in different channel shapes

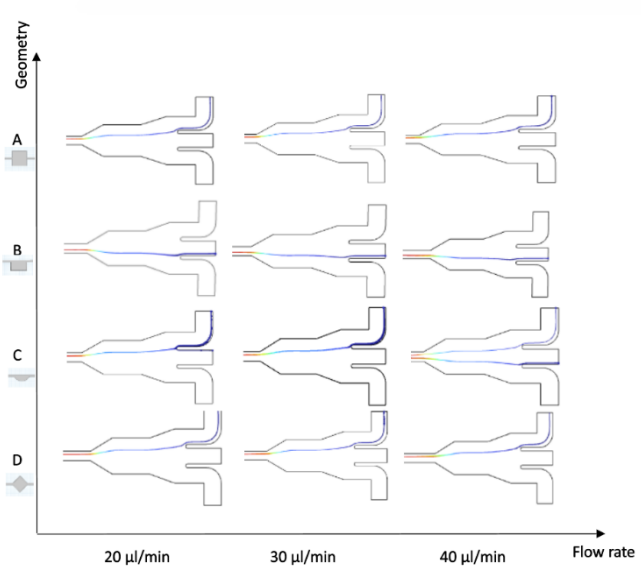

Figure 4.2.1: Channel outlets at 500 ppm PEO solution

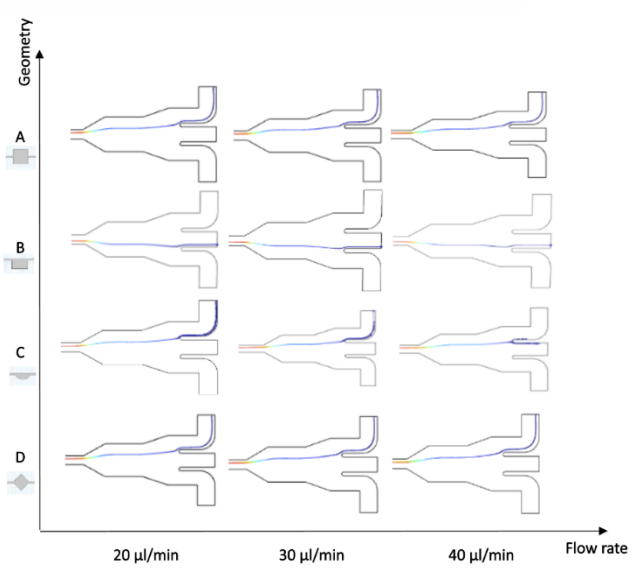

Figure 4.2.2: Channel outlets at 1000 ppm PEO solution

The figures 4.2.1 and 4.2.2 present a comparative analysis of the exit behavior of 4.8 µm particles at the end of microchannels featuring four distinct geometries-both side rectangle channel, rectangular channel, curved channel, and both side triangular channel-under two different concentrations of PEO solution: 500 ppm and 1000 ppm. The flow rates examined are 20, 30, and 40 µL/min, providing insight into how these parameters affect particle migration and focusing within viscoelastic microfluidic environments

For the 500 ppm PEO solution, the distribution of particle exits across the different channel geometries is relatively broad, indicating that the elastic forces present at this concentration are not strong enough to induce sharp particle focusing. In both side square channel and both side triangle channel, the complexity and sharp corners of the geometries create localized regions of low shear rate, which can guide particles toward specific exits, but the effect remains moderate at this lower PEO concentration. The square channel, with its more regular geometry, shows less pronounced particle migration, resulting in exits that are more evenly distributed. The curved channel, characterized by its smooth transitions, tends to produce a more gradual focusing effect, with particles displaying a slight preference for certain exits as the flow rate increases. When the PEO concentration is increased to 1000 ppm, the viscoelastic properties of the fluid become more prominent, leading to a marked enhancement in particle focusing behavior. In the both side square channel and both side triangle channel, the presence of strong elastic lift forces, especially at higher flow rates, results in a much narrower distribution of

particle exits, with most particles being directed toward specific outlets. This behavior is attributed to the intensified elastic effects in the low shear rate zones created by the channel geometry, which effectively steer particles along preferred streamlines. The square channel also exhibits improved focusing at 1000 ppm, but the effect is less dramatic compared to the more complex geometries. The curved channel, while still promoting some degree of particle migration, demonstrates a smoother and more continuous transition in exit distribution as the flow rate increases, reflecting the interplay between channel curvature and viscoelastic forces.

Overall, the figures clearly demonstrate that both the geometry of the microchannel and the concentration of the viscoelastic solution play critical roles in determining the exit path of suspended particles. Higher PEO concentrations and more intricate channel shapes, such as the both side square and both side triangle channels, significantly enhance particle focusing, resulting in more predictable and controllable exit distributions. This understanding is essential for the design of microfluidic systems aimed at efficient particle sorting, focusing, and manipulation, as it underscores the importance of tailoring both the fluid properties and channel architecture to achieve desired outcomes in lab-on-a-chip applications

4.3 Particle deviation at the end of straight channel.

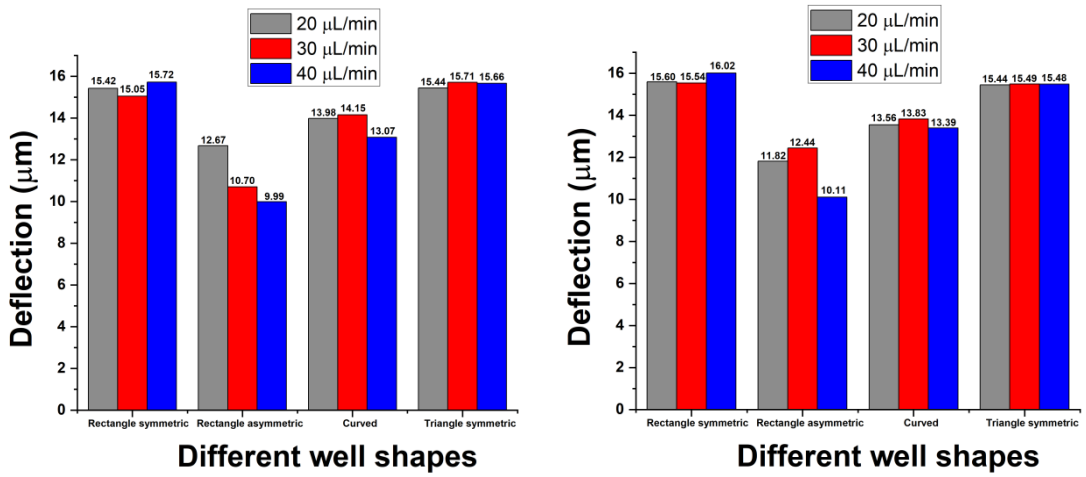

a) 500 ppm PEO b) 1000 ppm PEO

Figure 4.3 Average particle deviation at the end of straight channel with change in well shapes for a) 500 ppm PEO solution and b) 1000 ppm PEO solution.

When examining the average deviation of particles at the end of the straight section of the microchannel, the influence of both PEO concentration and well geometry becomes clear. At a lower PEO concentration of 500 ppm, as shown in Figure 4.3a, the data reveal that the rectangle symmetric and triangle symmetric wells consistently produce the highest average deviations, with values hovering around 15.4 to 15.7 μm across all tested flow rates. This suggests that these symmetric geometries are particularly effective at promoting lateral migration of particles, likely due to the formation of pronounced low shear rate zones and the generation of secondary flows within the channel.

In contrast, the rectangle asymmetric wells display a noticeable decrease in deviation as the flow rate increases, dropping from 12.67 μm at 20 μL/min to just under 10 μm at 40 μL/min. The curved wells also show a slight reduction in deviation with increasing flow rate, ranging from 13.98 μm down to 13.07 μm. These trends indicate that, at 500 ppm, the elastic forces present in the system are not yet strong enough to cause significant changes in particle trajectories as the flow rate increases. Instead, the geometry of the well plays a more dominant role in determining the extent of lateral migration.

When the PEO concentration is increased to 1000 ppm, as depicted in Figure 4.3b, the average deviation of particles rises for all channel geometries. The rectangle symmetric and triangle symmetric wells continue to stand out, with deviations remaining above 15 μm and reaching up to 16.02 μm in the rectangle symmetric case at the highest flow rate. This increase in deviation with higher PEO concentration highlights the enhanced viscoelastic effects at play, where stronger elastic lift forces are able to drive particles more effectively toward specific streamlines, resulting in greater lateral displacement.

Interestingly, the rectangle asymmetric wells at 1000 ppm show a peak deviation of 12.44 μm at 30 μL/min, but this value drops to 10.11 μm at 40 μL/min, mirroring the trend observed at the lower concentration. The curved wells also experience a modest increase in deviation, peaking at 13.83 μm at 30 μL/min before slightly decreasing at the highest flow rate. These results underscore the importance of both polymer concentration and channel geometry in shaping particle behavior within microfluidic systems

Overall, increasing the PEO concentration from 500 ppm to 1000 ppm amplifies the viscoelastic effects within the channel, resulting in greater and more consistent particle deviation, especially in the rectangle symmetric and triangle symmetric wells. The geometry

of the channel remains a crucial factor, with symmetric designs consistently yielding higher deviations and thus proving more effective for lateral migration and focusing of particles. Flow rate, on the other hand, has only a minor influence on deviation at both concentrations, as the deviations remain relatively stable across the tested range. This stability suggests that, under these conditions, viscoelastic forces are the dominant mechanism governing particle migration, overshadowing the effects of inertial forces.

4.4 Pressure variation across different channel geometries

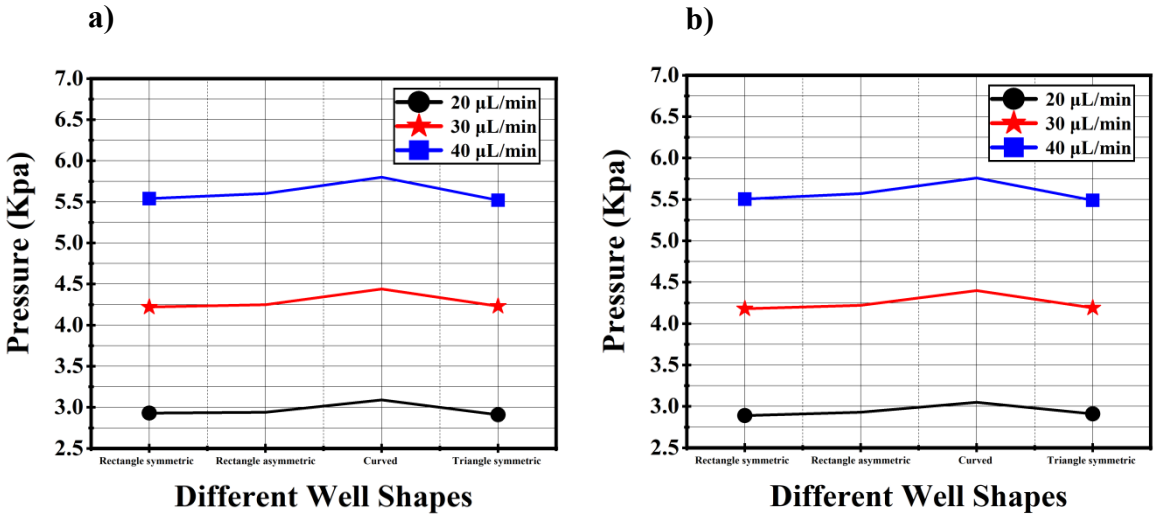

Figure 4.4: Pressure drop across different channel geometries for a) 500 ppm PEO solution and b) 1000 ppm PEO solution.

A closer look at the pressure drop data for the various microchannel geometries, as illustrated in Figures 4.4a and 4.4b, reveals how profoundly the shape of the wells influences the hydrodynamic resistance encountered by the viscoelastic fluid. At a flow rate of 20 µL/min, the pressure required to drive the fluid through the rectangle symmetric channel is approximately 2.8 kPa, while the rectangle asymmetric channel shows a slightly higher value, just above 3.0 kPa. The curved channel, with its smooth transitions, maintains a pressure drop similar to the rectangle symmetric case, also around 2.8 kPa. In contrast, the triangle symmetric channel matches the rectangle symmetric channel, reinforcing the trend that symmetric designs consistently yield lower pressure drops.

As the flow rate increases to 30 µL/min, the pressure drop rises across all geometries, but the differences between them become more pronounced. The rectangle symmetric and triangle

symmetric channels both exhibit pressure drops just under 3.5 kPa, while the rectangle asymmetric channel climbs to nearly 4.0 kPa. The curved channel remains close to the symmetric designs, with a pressure drop slightly above 3.5 kPa. At the highest tested flow rate of 40 μL/min, the rectangle symmetric and triangle symmetric channels maintain their lower pressure drops, both just above 3.5 kPa, whereas the rectangle asymmetric channel reaches nearly 4.5 kPa. The curved channel, again, stays in line with the symmetric geometries, with a pressure drop just under 4.0 kPa.

When the PEO concentration is increased to 1000 ppm, the overall pressure drops are higher, but the same pattern persists. At 20 μL/min, the rectangle symmetric and triangle symmetric channels both require about 5.5 kPa to sustain the flow, while the rectangle asymmetric channel demands a higher pressure, close to 6.0 kPa. The curved channel, as before, aligns with the symmetric designs, with a pressure drop of approximately 5.5 kPa. At 30 μL/min, the rectangle symmetric and triangle symmetric channels reach around 6.0 kPa, while the rectangle asymmetric channel peaks at nearly 6.5 kPa. The curved channel shows a slight increase, maintaining a pressure drop just above 6.0 kPa. At 40 μL/min, the rectangle symmetric and triangle symmetric channels both settle at about 5.5 kPa, while the rectangle asymmetric channel remains elevated, just under 6.0 kPa. The curved channel, consistent with previous observations, stays close to the symmetric designs.

These quantitative results make it clear that symmetric well shapes—whether rectangular, curved, or triangular—consistently facilitate smoother, more balanced flow paths, which in turn minimize abrupt expansions, contractions, and sharp corners. This design advantage reduces localized regions of high resistance and elastic stress, resulting in lower operational pressures. On the other hand, asymmetric channels disrupt the flow, leading to increased energy dissipation and a higher overall pressure drop. For microfluidic applications, this distinction is crucial: selecting symmetric well shapes not only reduces the pressure required to operate the device but also enhances the efficiency of particle manipulation in viscoelastic fluids, making these designs especially attractive for practical use.

4.5 Deviation across symmetric wells (rectangles and triangles) for variation in number of wells

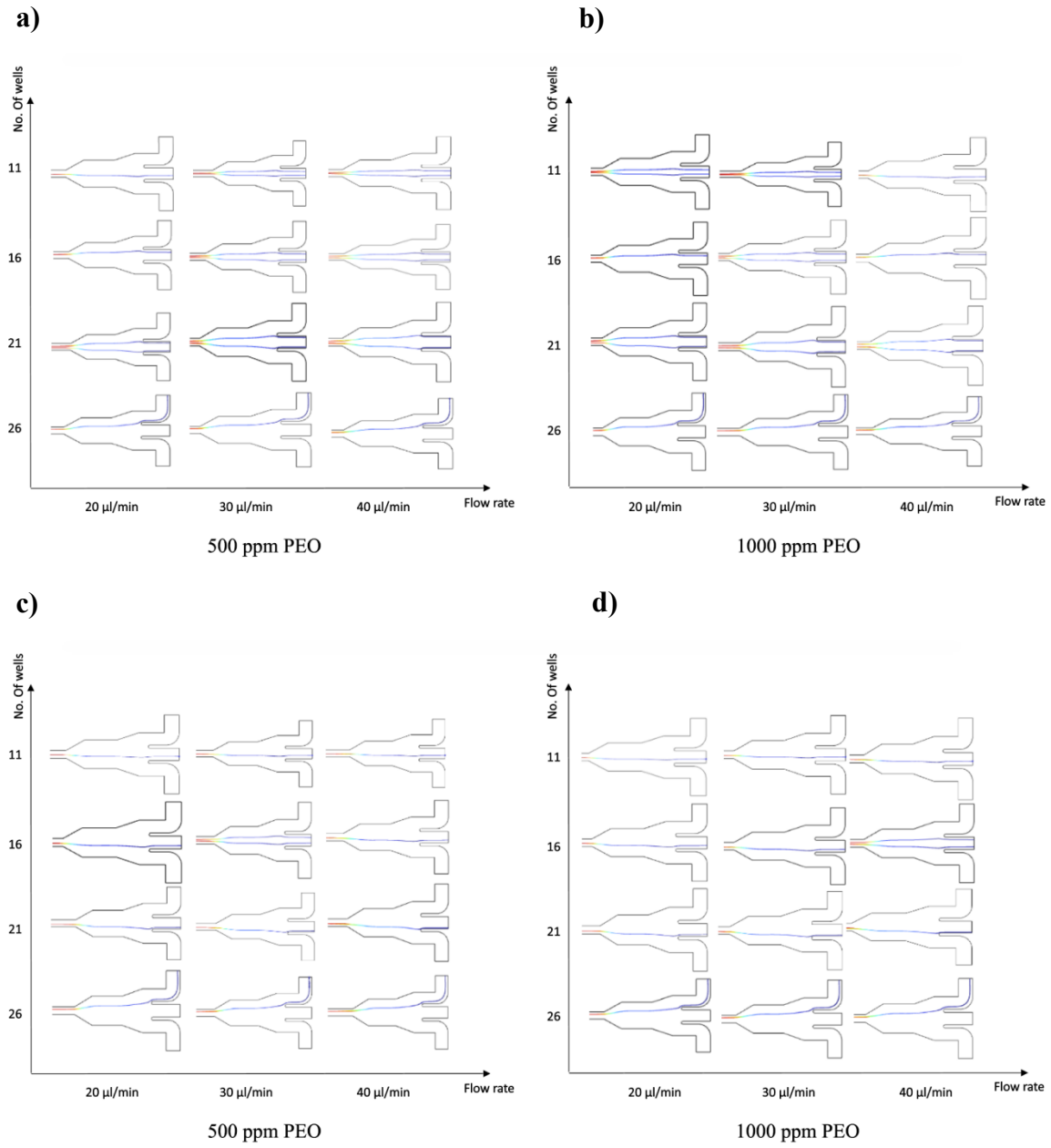

Figure 4.5: Deviation of particles at symmetric channel with change in number of wells and flow rate for - a) both side rectangular wells and 500 ppm PEO solution, b) both side rectangular wells and 1000 ppm PEO solution, c) both side triangular wells and 500 ppm PEO solution, and d) both side triangular wells and 1000 ppm PEO solution.

When examining the data for symmetric microchannels with rectangular and triangular wells on both sides, a clear pattern emerges regarding how the number of wells influences particle deviation, especially when considering different PEO concentrations. As more wells are added along the channel, particles experience a greater cumulative effect from the repeated geometric disturbances, which leads to a more pronounced lateral migration by the time they reach the end of the channel. This effect is evident in both rectangular and triangular well configurations, but the magnitude and rate of increase in deviation can differ based on the well shape and the viscoelasticity of the fluid.

For channels with symmetric rectangular wells, each additional well acts almost like a gentle nudge, incrementally steering the particles further away from their original streamline. At lower PEO concentrations, these nudges are relatively subtle, and the overall deviation remains modest even as the number of wells increases. However, as the PEO concentration rises, the viscoelastic forces within the fluid become much stronger, amplifying the influence of each well. This means that with a higher number of wells, especially at elevated PEO concentrations, the particles are guided more effectively toward the channel periphery, resulting in a much larger average deviation.

The effect is even more pronounced in channels with symmetric triangular wells. The sharper geometry of these wells creates more intense regions of low shear and secondary flows, which, when combined with the viscoelastic properties of the fluid, act to push the particles even further laterally. Here, the increase in deviation with each additional well is steeper, and the cumulative effect is quite dramatic at higher PEO concentrations. It's almost as if each triangular well gives the particles a stronger push, and with more wells, this effect compounds rapidly, leading to significant lateral migration by the time the particles exit the channel1.

In essence, the number of wells in a microchannel act as a powerful lever for controlling particle deviation, especially when working with viscoelastic fluids. The more wells present, the greater the opportunity for the fluid's elastic forces to interact with the channel geometry, resulting in enhanced particle migration. This relationship is particularly valuable for microfluidic applications where precise control over particle positioning is required, such as in cell sorting or particle focusing. By thoughtfully increasing the number of wells, researchers can achieve higher levels of particle deviation, tailoring the system to their specific needs and making the most of the unique interplay between channel design and fluid mechanics

4.6 Particle deviation at the end of straight channel for increasing number of wells

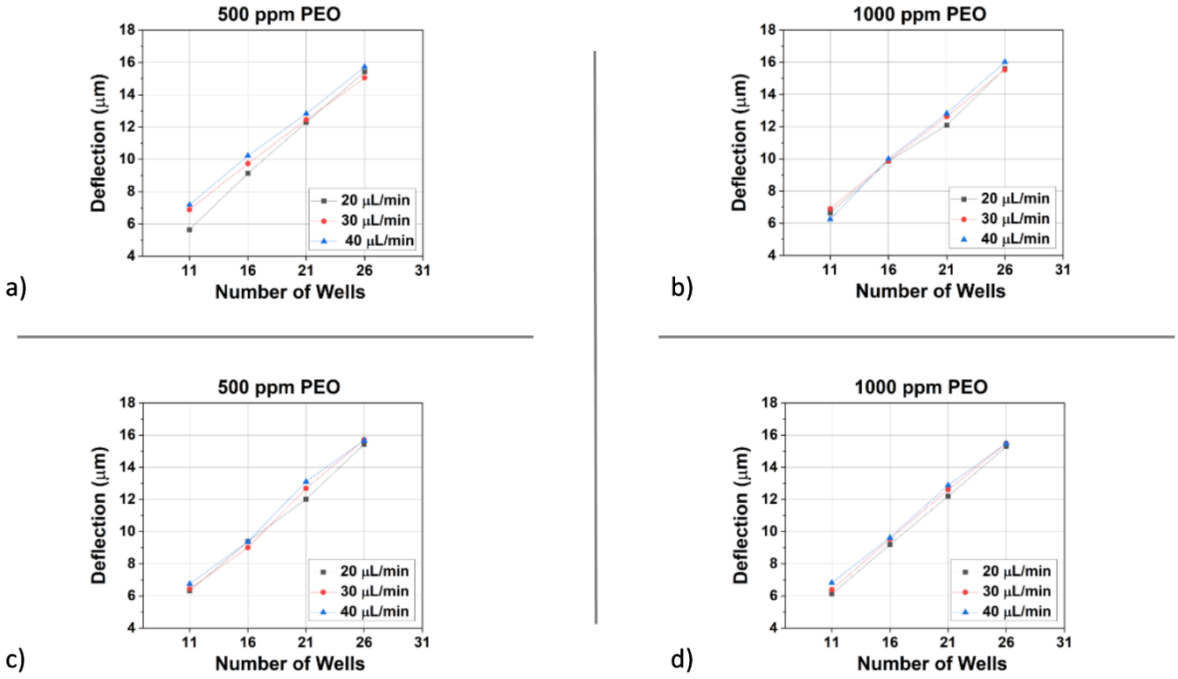

Figure 4.6: Deflection versus number of wells. a) symmetric channel with rectangular wells at 500 ppm PEO solution. b) symmetric channel with rectangular wells at 1000 ppm PEO solution. c) symmetric channel with triangular wells at 500 ppm PEO solution. Figure d) symmetric channel with triangular wells at 1000 ppm PEO solution.

The influence of the number of wells on particle deviation at the end of the straight microchannel is distinctly captured in the data for symmetric channels with rectangular and triangular wells on both sides, under two different PEO concentrations—500 ppm and 1000 ppm. For channels featuring rectangular wells (Figures a and b), the trend is clear: as the number of wells increases, the average lateral deviation of particles also rises. At the lower PEO concentration of 500 ppm, this increase is steady but relatively moderate. Specifically, when the number of wells grows from 11 to 31, the average particle deviation increases from approximately 7 μm to about 15.5 μm across the tested flow rates (20, 30, and 40 μL/min). This gradual rise suggests that each additional well contributes incrementally to pushing particles further from their original streamline, but the viscoelastic forces at this concentration are not yet strong enough to cause dramatic shifts in particle trajectories.

When the PEO concentration is elevated to 1000 ppm, the effect of increasing the number of wells becomes much more pronounced. The data show that as the number of wells increases

from 11 to 31, the average deviation climbs more sharply, reaching values close to 16 μm at the highest flow rates. This steeper increase reflects the enhanced elasticity of the fluid, which amplifies the cumulative influence of multiple wells. The stronger viscoelastic forces at this concentration more effectively drive particles laterally, resulting in significantly greater migration by the time they exit the channel.

A similar but even more striking pattern emerges in channels with triangular wells on both sides (Figures c and d). The sharper geometry of the triangular wells appears to intensify the effect of each additional well, especially at the higher PEO concentration. At 500 ppm, the average deviation increases from around 7 μm with 11 wells to nearly 16 μm with 31 wells, showing a more substantial rate of increase compared to the rectangular wells. This suggests that the triangular shape, with its sharper angles and more pronounced flow disturbances, enhances the lateral displacement of particles even at moderate viscoelastic forces.

At 1000 ppm PEO, this effect becomes dramatically more evident. The average deviation rises steeply as the number of triangular wells increases, reaching values slightly above 16 μm at the highest flow rates and well counts. The data indicate that each additional triangular well significantly boosts particle deviation, leading to a much steeper and more pronounced rise in lateral migration compared to the rectangular well channels. This highlights the combined impact of well geometry and fluid elasticity in shaping particle trajectories within microfluidic systems.

In summary, the number of wells plays a crucial role in determining particle deviation, with more wells leading to greater lateral migration. This effect is amplified by higher PEO concentrations, which strengthen viscoelastic forces, and by the sharper geometry of triangular wells, which more effectively disrupt flow and enhance particle displacement. These insights are vital for optimizing microchannel designs aimed at precise particle focusing and separation, emphasizing the importance of both structural and fluidic parameters in achieving desired outcomes.

4.7 Effect of further extension of the number of wells on a Symmetric channel

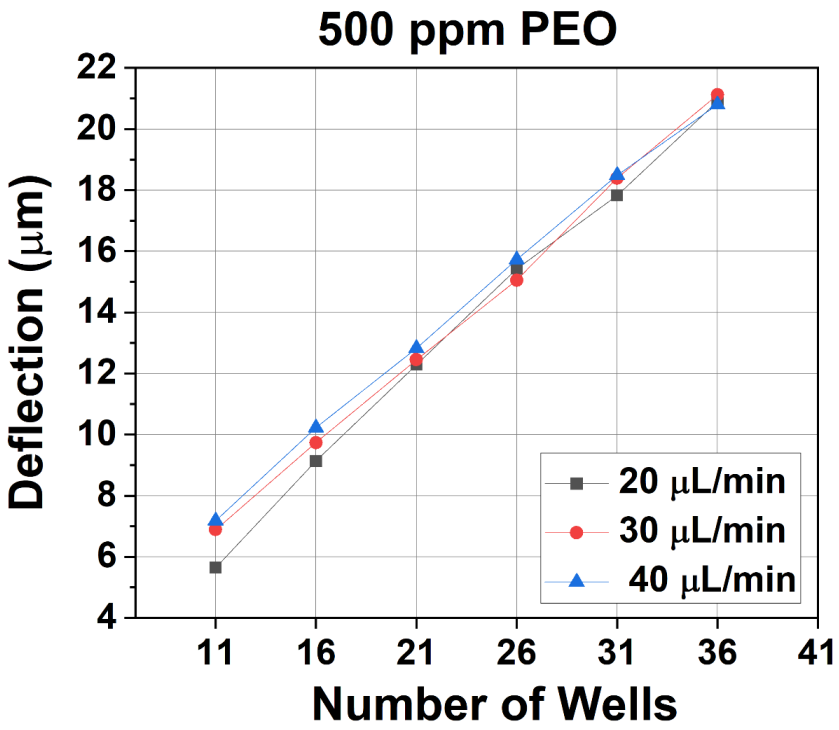

Figure 4.7: Effect of well count on particle deflection at 500 ppm PEO for varying flow rates.

The simulation results provide a detailed picture of how both the number and geometry of wells influence particle deviation in symmetric microchannels under viscoelastic flow conditions. As the number of rectangular wells increases from 11 to 26, the simulations show a steady and almost linear increase in average particle deviation. For example, at a flow rate of 20 µL/min and a PEO concentration of 500 ppm, the simulated average deviation rises from around 7 µm with 11 wells to approximately 15 µm with 26 wells. This upward trend is consistent at higher flow rates, with deviations approaching 16 µm at 40 µL/min for the same number of wells. When the PEO concentration is increased to 1000 ppm, the simulations predict an even steeper climb in deviation as additional wells are introduced, highlighting the significant role of enhanced viscoelastic forces in promoting lateral particle migration.

However, when the simulations extend the number of wells beyond 26-up to 36 the increase in deviation continues but at a noticeably reduced rate. For instance, at 500 ppm and the highest tested flow rate, the deviation grows from about 15 µm at 26 wells to just over 20 µm at 36 wells. This slower rise suggests a saturation effect within the simulated system: while each new well still contributes to lateral migration, its incremental impact diminishes as particles

approach the microchannel boundaries or reach equilibrium positions where elastic, viscous, and inertial forces balance out. The viscoelastic focusing effect, while still present, becomes less efficient with each additional well past this threshold.

This simulated plateau in particle deviation has important implications for microfluidic design. The results indicate that increasing the number of wells is an effective strategy for enhancing particle migration up to a certain point, but beyond roughly 26 wells, further additions yield only marginal gains. This insight is valuable for optimizing channel designs in silico, as it suggests there is an optimal range for the number of wells that balances efficient particle focusing with practical considerations such as device complexity and simulated pressure drop.

These trends from the simulations are consistent with observations in recent computational studies, where similar saturation effects have been reported in microchannels featuring periodic geometric disturbances, especially at moderate to high polymer concentrations. In summary, the simulation data demonstrate that increasing the number of rectangular wells in a symmetric microchannel significantly enhances particle deviation up to about 26 wells, after which the effect plateaus. This behavior reflects the interplay between channel geometry and viscoelastic migration forces in the simulated environment, and should guide the computational optimization of microfluidic devices for particle focusing and sorting applications

Chapter 5

Conclusion and Future Scope

Through a detailed series of simulations, this thesis paints a comprehensive picture of how microparticles behave in viscoelastic flows within microchannels of varying geometries. The data make it clear that both the shape and number of wells, as well as the viscoelastic properties of the fluid, are pivotal in determining the extent of particle migration. Symmetric well geometries—especially rectangular and triangular designs-consistently facilitate greater lateral deviation, with average values reaching up to 16.0 μm at 1000 ppm PEO and 40 μL/min. In contrast, asymmetric geometries lag behind, with deviations dropping to as low as 9.99 μm under comparable conditions.

The influence of the number of wells is equally significant. Up to about 26 wells, each additional well contributes meaningfully to particle deviation, but beyond this threshold, the effect begins to saturate. For example, at 500 ppm and 40 μL/min, the deviation rises from 15 μm at 26 wells to just over 20 μm at 36 wells, indicating diminishing returns for further geometric complexity. This plateau suggests that there is an optimal range for the number of wells, beyond which additional features do not substantially enhance focusing performance.

Pressure drop analysis adds another layer of insight, showing that symmetric channels consistently require less energy to operate, maintaining pressure drops in the range of 2.8 kPa at 500 ppm and 20 μL/min and 5.5 kPa at 1000 ppm and 40 μL/min, while asymmetric channels can demand nearly 3.1 kPa and 5.75 kPa, respectively, at the highest flow rates. Taken together, these findings underscore the importance of thoughtful microchannel design in applications where precise particle focusing and sorting are required. By carefully tuning the number and geometry of wells and selecting the appropriate polymer concentration, it is possible to achieve efficient, passive particle manipulation without incurring unnecessary pressure losses. The quantitative trends uncovered in this thesis not only deepen our understanding of viscoelastic microfluidics but also offer practical guidelines for the next generation of high-performance microfluidic devices in biomedical and analytical fields.

Future Scope:

While this study successfully demonstrates the influence of microchannel geometry and viscoelastic fluid properties on microparticle migration through numerical simulations, there

remains considerable scope for further research. A key next step would be to fabricate the proposed channel geometries and conduct experimental validation of the simulated results. This would not only confirm the predictive accuracy of the current model but also provide insights into any discrepancies arising from real-world factors such as fabrication tolerances, particle variability, or flow instabilities.

In addition, future work could explore a wider range of particle sizes and shapes, including deformable biological cells, to assess how these parameters influence migration patterns in viscoelastic media. Investigating the combined effects of multiple forces—such as electrokinetic or magnetophoretic forces in conjunction with viscoelastic flows—may also open new avenues for enhancing separation efficiency and selectivity.

Moreover, optimizing channel designs for high-throughput applications and integrating them into complete lab-on-a-chip platforms could significantly advance their practical utility in clinical and diagnostic settings. Finally, extending the simulations to three-dimensional models and transient flow conditions would help in better understanding complex particle trajectories and improving the overall robustness of the microfluidic system design.

References

[1] D. Di Carlo, “Inertial microfluidics,” 2009, *Royal Society of Chemistry*. doi: 10.1039/b912547g.

[2] G. D’Avino and P. L. Maffettone, “Particle dynamics in viscoelastic liquids,” Jan. 01, 2015, *Elsevier*. doi: 10.1016/j.jnnfm.2014.09.014.

[3] J. Nam, H. Lim, D. Kim, H. Jung, and S. Shin, “Continuous separation of microparticles in a microfluidic channel via the elasto-inertial effect of non-Newtonian fluid,” *Lab Chip*, vol. 12, no. 7, pp. 1347–1354, Apr. 2012, doi: 10.1039/c2lc21304d.

[4] G. M. Whitesides, “The origins and the future of microfluidics,” Jul. 27, 2006. doi: 10.1038/nature05058.

[5] S. N. Bhatia and D. E. Ingber, “Microfluidic organs-on-chips,” 2014, *Nature Publishing Group*. doi: 10.1038/nbt.2989.

[6] D. W. Inglis, J. A. Davis, R. H. Austin, and J. C. Sturm, “Critical particle size for fractionation by deterministic lateral displacement,” *Lab Chip*, vol. 6, no. 5, pp. 655–658, 2006, doi: 10.1039/b515371a.

[7] A. Sharei *et al.*, “A vector-free microfluidic platform for intracellular delivery,” *Proc Natl Acad Sci U S A*, vol. 110, no. 6, pp. 2082–2087, Feb. 2013, doi: 10.1073/pnas.1218705110.

[8] E. J. Lim *et al.*, “Inertio-elastic focusing of bioparticles in microchannels at high throughput,” *Nat Commun*, vol. 5, Jun. 2014, doi: 10.1038/ncomms5120.

[9] S. Hettiarachchi *et al.*, “Viscoelastic microfluidics for enhanced separation resolution of submicron particles and extracellular vesicles,” *Nanoscale*, vol. 16, no. 7, pp. 3560–3570, Jan. 2024, doi: 10.1039/d3nr05410a.

[10] J. Zhou and I. Papautsky, “Viscoelastic microfluidics: progress and challanges,” Dec. 01, 2020, *Springer Nature*. doi: 10.1038/s41378-020-00218-x.

[11] D. Yuan *et al.*, “Investigation of particle lateral migration in sample-sheath flow of viscoelastic fluid and Newtonian fluid,” *Electrophoresis*, vol. 37, no. 15–16, pp. 2147–2155, Aug. 2016, doi: 10.1002/elps.201600102.

[12] S. Hazra, A. Nath, S. K. Mitra, and A. K. Sen, “Dynamics of rigid particles in a confined flow of viscoelastic and strongly shear-thinning fluid at very small Reynolds numbers,” *Physics of Fluids*, vol. 33, no. 5, May 2021, doi: 10.1063/5.0046729.

[13] D. Yuan *et al.*, “Continuous plasma extraction under viscoelastic fluid in a straight channel with asymmetrical expansion-contraction cavity arrays,” *Lab Chip*, vol. 16, no. 20, pp. 3919–3928, 2016, doi: 10.1039/c6lc00843g.

[14] L. L. Fan *et al.*, “Enhanced viscoelastic focusing of particle in microchannel,” *Electrophoresis*, vol. 41, no. 10–11, pp. 973–982, Jun. 2020, doi: 10.1002/elps.201900397.

[15] T. Wang, D. Yuan, W. Wan, and B. Zhang, “Numerical Study of Viscoelastic Microfluidic Particle Manipulation in a Microchannel with Asymmetrical Expansions,” *Micromachines (Basel)*, vol. 14, no. 5, May 2023, doi: 10.3390/mi14050915.

[16] D. Yuan *et al.*, “Continuous plasma extraction under viscoelastic fluid in a straight channel with asymmetrical expansion-contraction cavity arrays,” *Lab Chip*, vol. 16, no. 20, pp. 3919–3928, 2016, doi: 10.1039/c6lc00843g.

[17] S. Hazra, S. K. Mitra, and A. K. Sen, “Cross-stream migration of droplets in a confined shear-thinning viscoelastic flow: Role of shear-thinning induced lift,” *Physics of Fluids*, vol. 32, no. 9, Sep. 2020, doi: 10.1063/5.0016534.

[18] H. Lim, S. M. Back, M. H. Hwang, D. H. Lee, H. Choi, and J. Nam, “Sheathless high-throughput circulating tumor cell separation using viscoelastic non-Newtonian fluid,” *Micromachines (Basel)*, vol. 10, no. 7, Jul. 2019, doi: 10.3390/mi10070462.

[19] E. S. Asmolov, “The inertial lift on a spherical particle in a plane poiseuille flow at large channel Reynolds number,” *J Fluid Mech*, vol. 381, pp. 63–87, Feb. 1999, doi: 10.1017/S0022112098003474.

[20] S.-C. Xue, N. Phan-Thien, and R. I. Tanner, “Numerical study of secondary flows of viscoelastic fluid in straight pipes by an implicit finite volume method,” 1995.

[21] A. N. Brooks and T. J. R. Hughes, “Streamline Upwind/Petrov-Galerkin formulations for CON~C~ON coated flows with particular emphasis on the incompressible Naview-Stokes equations,” 1982.

[22] J. M. Marchal and M. J. Crochet, “Hermitun finite elements for calculating viscoelastic flow,” Elsevier science Publishers B.V, 1986.

[23] J. M. Marchal and M. J. Crochet, “A new mixed finite element for calculating viscoelastic flow,” 1987.